PFC/RR-93-7

ITER/US/93/EV-MAG/A.
Radovinsky/11.9/1

Joule Heating of the ITER TF Cold Structure
Effects of Vertical Control Coil Currents and ELMS

A. Radovinsky and R.D. Pillsbury, Jr.
November 9, 1993

Plasma Fusion Center
Massachusetts Institute of Technology
Cambridge, Massachusetts 02139 USA

Supported under US DOE Grant DE-FC02-93-ER-54186

Table of Contents

List of Figures

List of Tables

1.0 Introduction and Summary

The toroidal field coil and support structures for ITER are maintained at cryogenic temperatures. The time-varying currents in the poloidal field coil system will induce eddy currents in these structures. The associated Joule dissipation will cause local heating and require heat removal which will show up as a load on the cryogenic system.

Studies of Joule heating of the ITER TF cold structure (TFCS) due to the currents in the poloidal field coil system are presented. The two regimes considered in this study are the plasma vertical stability control and the Edge Loss Mode (ELM) events. The 3-D, thin-shell, eddy current program, EDDYCUFF [1], was used to analyze the eddy currents and Joule losses in the cold structure. The current versus time scenarios were defined by [4-12].

Four control coil options were studied. All schemes use coils external to the TF cold structure. The four options are:

(1a) in which coils PF2 and PF7 are active,
(1b) in which all the coils PF2-PF7 are active,
(2) in which PF3 and PF5 are used, and
(3) in which a pair of coils separate from the PF system is used.

Analyses of power depositions during the plasma vertical stability control were performed for each of the four options. For each of these options three different recovery times were assumed. The times were 3, 1, and 1/3 seconds. Option #1a showed the minimum power deposition in the TF cold structure.

Sets of four sequential ELMs, as well as isolated ELMs have been studied for various sets of active PF coils. The results showed that the lowest average power dissipation in the TF cold structure occurs when a subset of PF2 and PF7 are active, and all the other PF coils are passive.

The general conclusion is that to minimize power dissipation in the TF cold structure it is preferable that only coils PF2 and PF7 are active. The other coils (PF3-PF6) should be passive and driven by a condition of constant flux. It is recommended in particular, that coils PF3 and PF5 be allowed to change currents to conserve flux, since they provide the maximum shielding of the TFCS from the fields caused by the active coils. It is highly undesirable to use any of the coils close to the TFCS (PF3-PF6) as active coils.

2.0 Model

The program EDDYCUFF was used in these analyses. EDDYCUFF assumes that the conducting medium is a shell which is thin relative to the skin depth. This implies a uniform distribution of current density through the thickness of the material. This also implies that there is no current flow perpendicular to the plane of the shell.

The TF cold structure (TFCS) modeled in the study consists of six segments. One segment is shown in Fig. 2.0-1. EDDYCUFF can take into account the symmetry of the structure as well as the symmetry of the eddy current patterns. Thus, only one half of a 1/6-th segment of the entire structure was included in the model, as shown in Fig. 2.0-2. The model is symmetric with respect to the plane Y=0. As is shown below, it is essential to take into account the shielding effect of the vacuum vessel (VV) and the blanket (BL). These elements were also included in the model if not specified differently. The meshes of these structural elements are shown separately in Fig. 2.0-3.

The bolted joints of the TF cold structure were modeled by the boundary condition for an insulated edge. The dimensions of the model correspond to [2]. The resistivity of the TF cold structure material is $5*10^{-7}$ ohm*m.

The vacuum vessel and the blanket were modeled as toroidal segments with boundary conditions permitting current flow in the circumferential direction. The resistivity was modified to produce a toroidal resistance of 10 $\mu\Omega$.

The dimensions of the PF coils involved in the study are listed in Table 2.0-1, unless specified below. They are based on [3]. All the dimensions are the same as in the cited document except for the radii of the PF4 and PF5 coils which have been increased to provide a 15 cm gap between the inner surface of the coils and the outer bore of the TF cold structure.

3.0 Joule Heating of the ITER TF Cold Structure due to the Vertical Control Coil Currents

The analysis of power deposition during the plasma vertical stability control shows that Option #1a, in which coils PF2 and PF7 are active, dissipates less average power in the TF cold structure than either Option #1b, in which all the peripheral coils, PF2-PF7, are active, or Option #2, in which PF3 and PF5 are used, or Option #3, in which a pair of coils separate from the PF system is used.

3.1 Current versus Time Scenarios

The current versus time scenarios were defined as follows.

Option #1a:

Option #1a is defined by [4]. The three cases considered correspond to the three current versus time scenarios (shown in Figs. 3.1-1.a - 3.1-1.c) with recovery times t_r=3, 1 and 1/3 seconds, respectively. Coils PF2 and PF7 are active; all the other peripheral PF coils (PF3-PF6) are passive and maintain constant flux; currents in PF1 are constant.

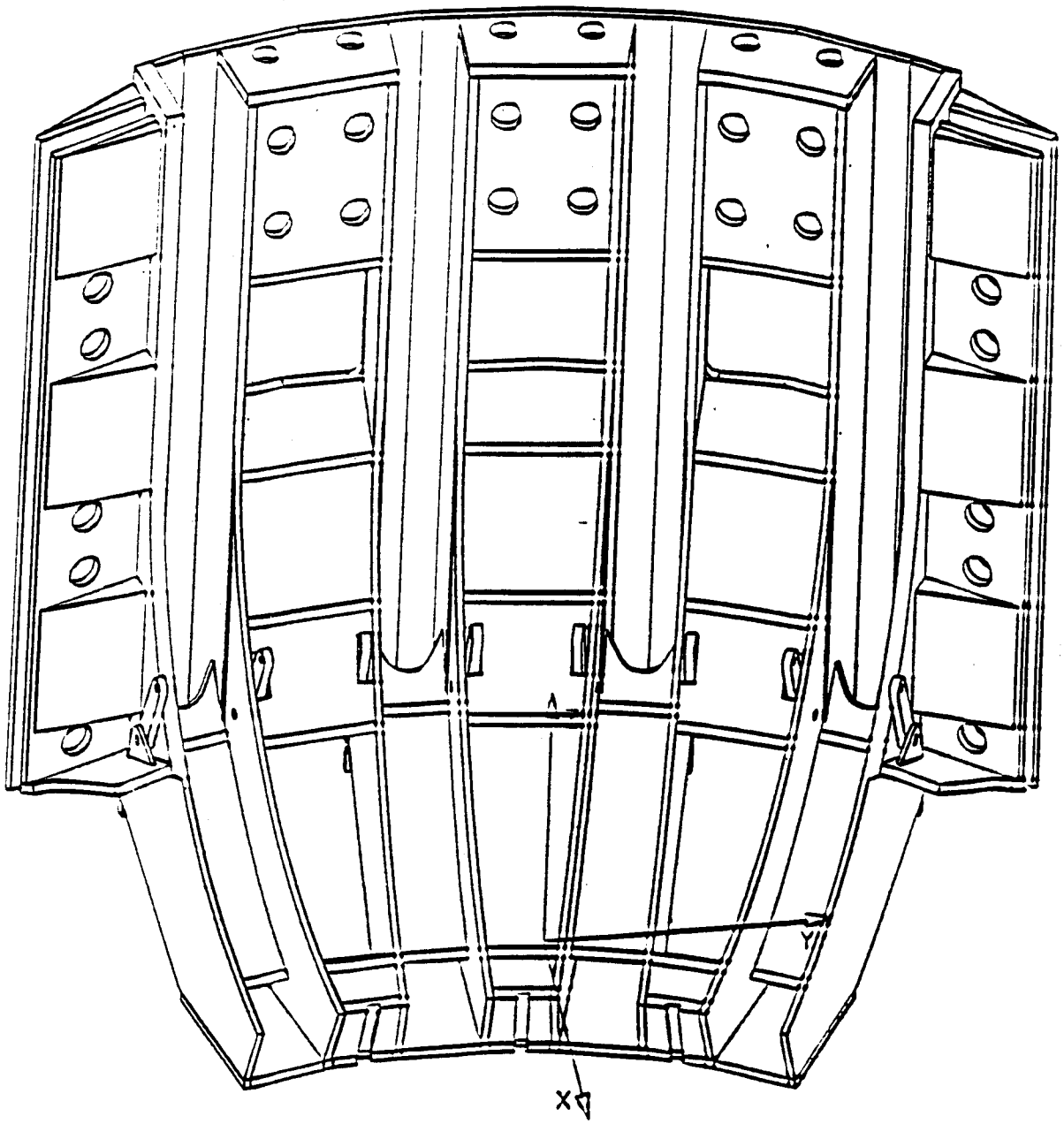

Fig. 2.0-1 One sixth of the TF cold structure

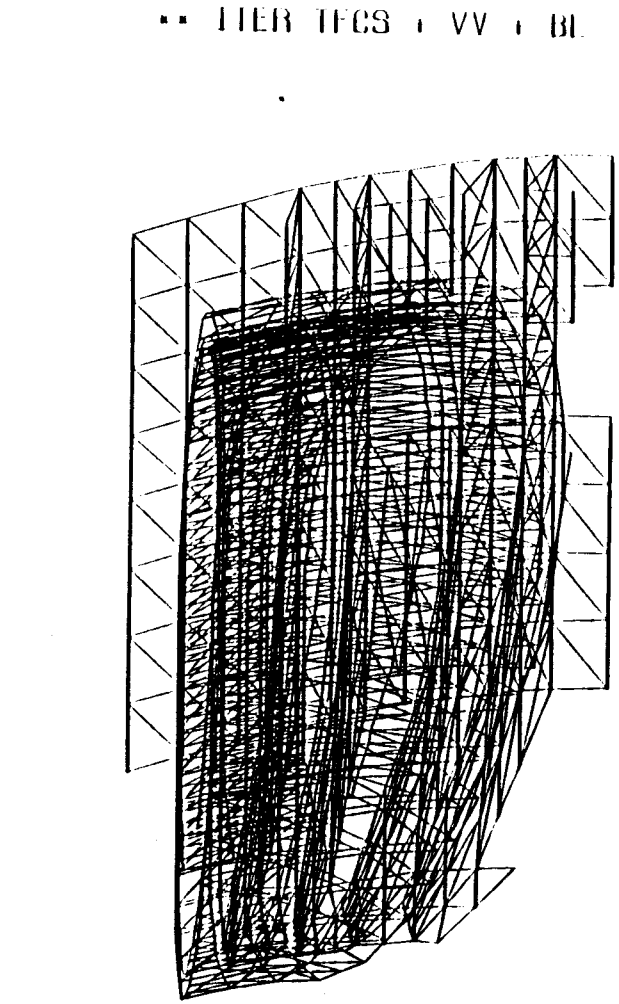

Fig. 2.0-2 The finite element model

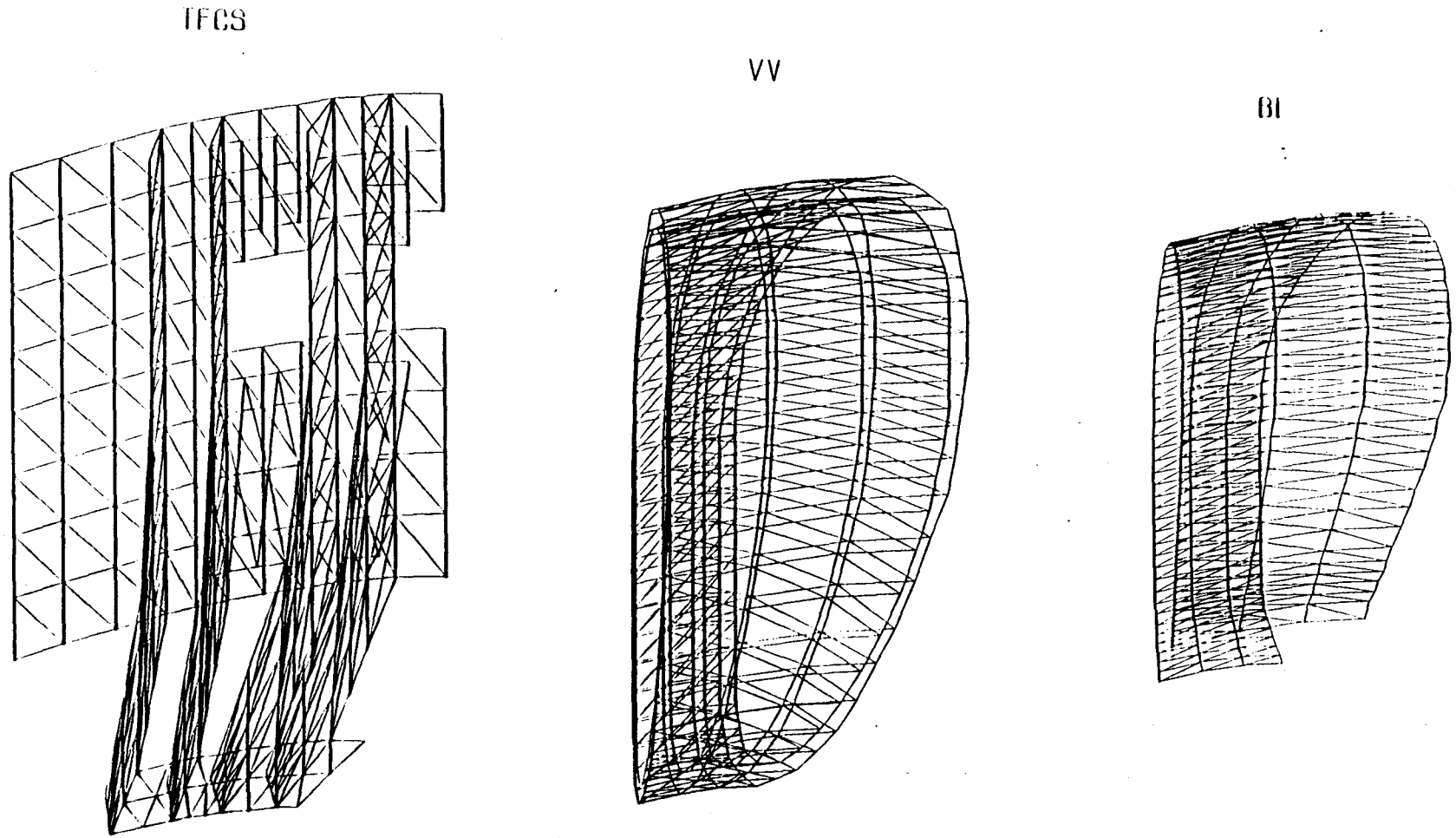

Fig. 2.0-3 Structural elements models

Table 2.0-1 Coil Dimensions

Coil	Rc (m)	Zc (m)	dR (m)	dZ (m)
PF1	2.498	0.000	0.775	12.120
PF2	5.947	9.981	1.098	1.161
PF3	13.017	7.197	1.000	0.537
PF4	15.365	-2.445	1.000	0.745
PF5	15.463	-5.745	1.196	1.027
PF6	9.650	-9.635	1.098	1.161
PF7	5.184	-9.485	1.098	1.161

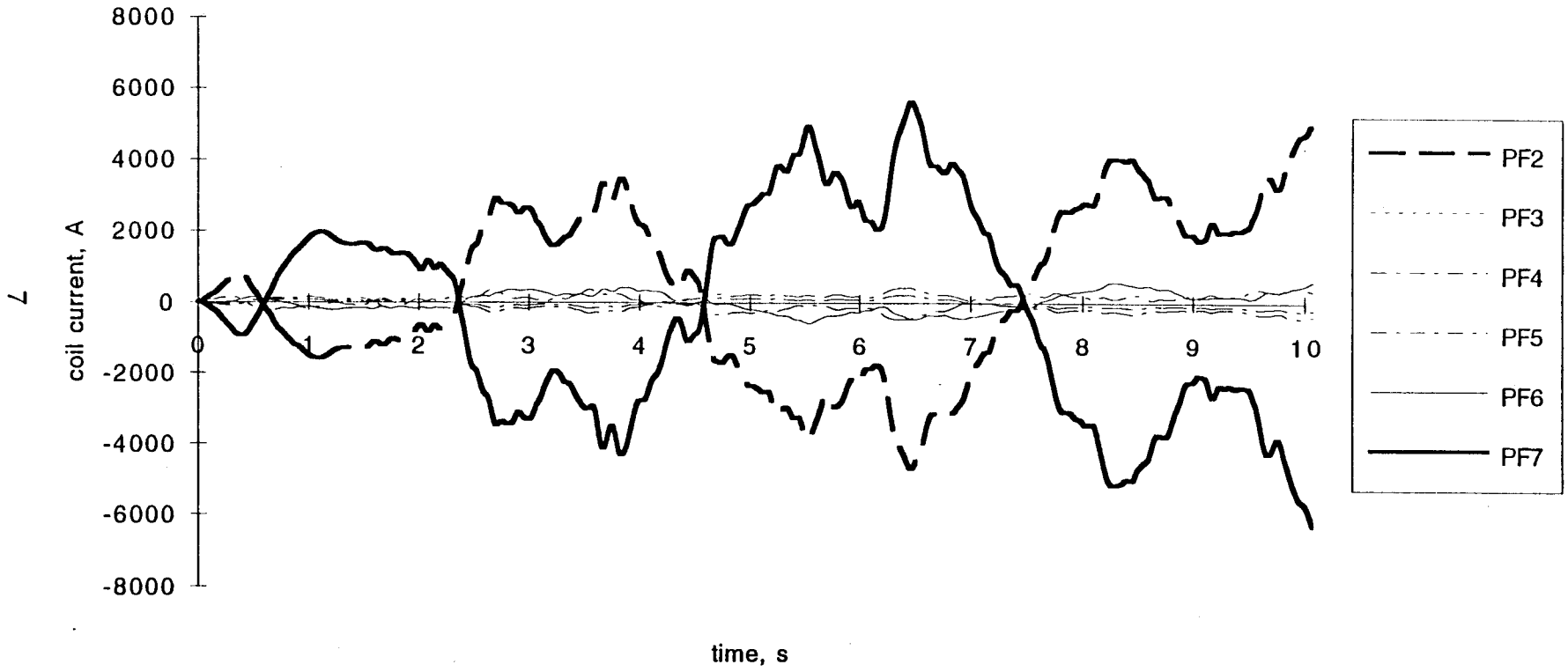

Fig. 3.1-1.a Vertical control coils current simulation, t_r=3 s, Opt.#1a

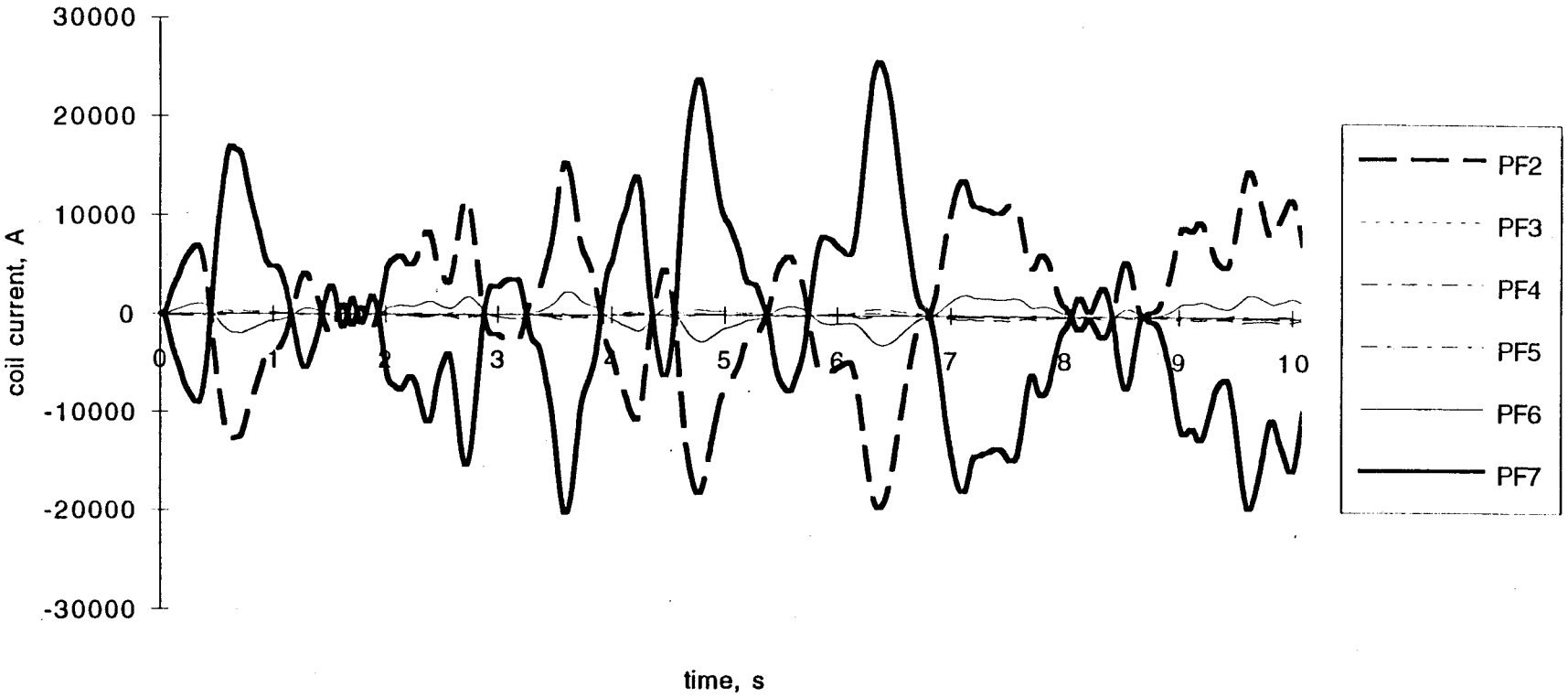

Fig. 3.1-1.b Vertical control coils current simulation, t_r=1 s, Opt.#1a

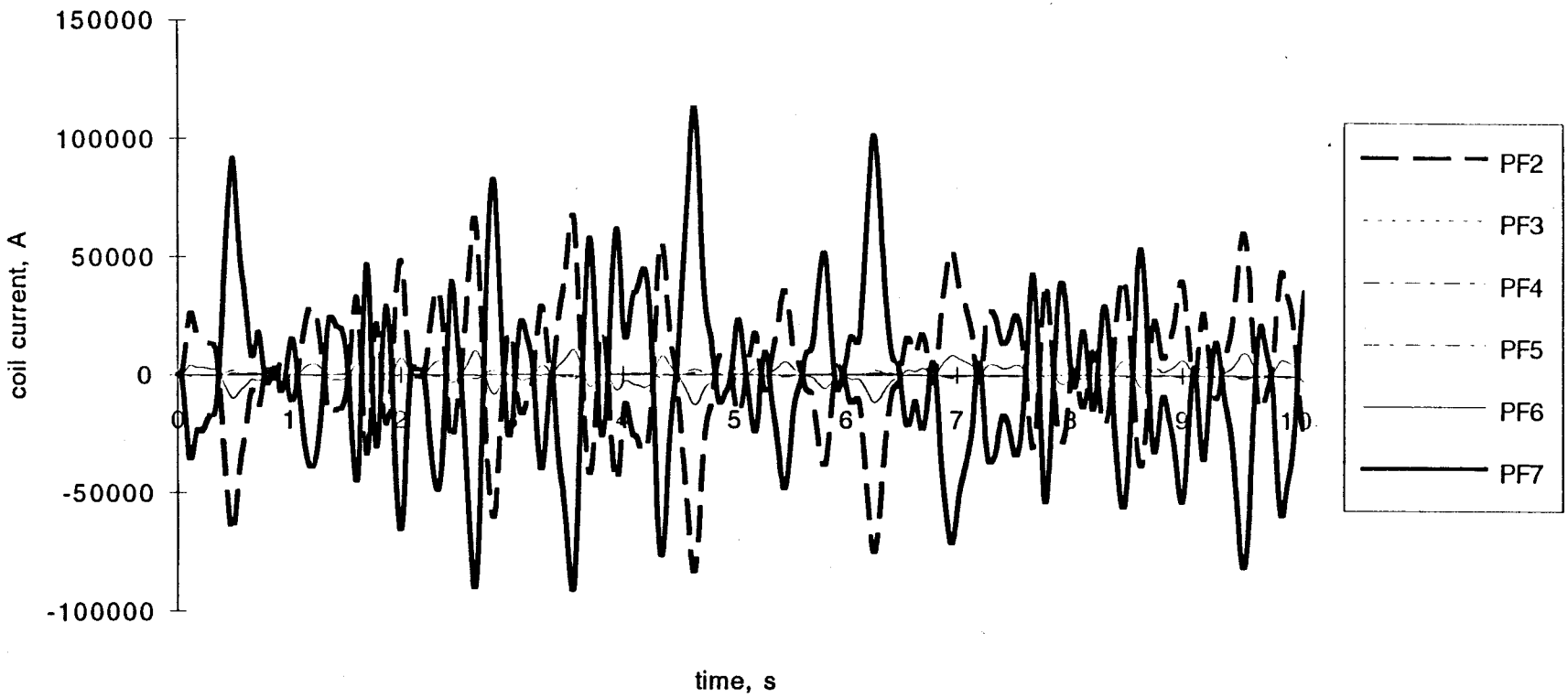

Fig. 3.1-1.c Vertical control coils current simulation, t_r=1/3 s, Opt.#1a

Option #1b:

Option #1b is defined by [5]. The three cases considered correspond to the three current versus time scenarios (shown in Figs. 3.1-2.a - 3.1-2.c) with recovery times t_r=3, 1 and 1/3 seconds, respectively. Peripheral coils PF2-PF7 are active, currents in PF1 are constant.

Option #2:

Option #2 is defined by [6]. The three cases considered correspond to the three current versus time scenarios (shown in Figs. 3.1-3.a - 3.1-3.c) with recovery times t_r=3, 1 and 1/3 seconds, respectively. A subset of PF3 and PF5 is used here. The dimensions of the coils were different from those in Table 1, and were defined as in the task description as follows:

PF3: R=13.017 m, Z=6.702 m, dR=0.565 m, dZ=0.160 m;
PF5: R=15.193 m, Z=-5.228 m, dR=0.785 m, dZ=0.116 m.

The currents in the two coils are opposite to each other. All the other PF coils maintain constant currents.

Option #3:

Option #3 is defined by [7]. The three cases considered correspond to the three current versus time scenarios (shown in Figs. 3.1-4.a - 3.1-4.c) with recovery times t_r=3, 1 and 1/3 seconds, respectively. In this option the vertical control coils were modeled by two solenoids of R=15.193 m, dR=dZ=0.05 m, placed at Z=+7.345/-4.035 m. The currents in the two coils are opposite to each other. The vertical control coils are separate from the main PF coils, and are outside the vacuum vessel as described in the task description. The currents in the PF coils are held constant.

The magnetic fields caused by the PF coils due to the normal scenario were not taken into account in these studies.

3.2 Joule Heating of the TFCS

The Joule losses for the three cases have been calculated. The power dissipation in the entire TF cold structure versus time is shown in Figs. 3.2-1.a - 3.2-1.c for Option #1a, Figs. 3.2-2.a - 3.2-2.c for Option #1b, Figs. 3.2-3.a - 3.2-3.c for Option #2, and Figs. 3.2-4.a - 3.2-4.c for Option #3, respectively.

The finite element model used in Options #2 and #3 included only the TF cold structure, whereas the model used for Options #1a and #1b also included the VV and the BL. An analysis performed for Options #2 and #3 showed that such simplification of the model has a negligible effect on the calculated power dissipated in the TFCS, whereas in Options #1a and #1b such simplification would cause a consistent error. Figure 3.2-2.a shows a comparison of power depositions in the TF cold structure for Option #1a (t_r=3 s) obtained using two different finite element models: the one described above which includes the VV and the BL (solid line), and a model taking into account

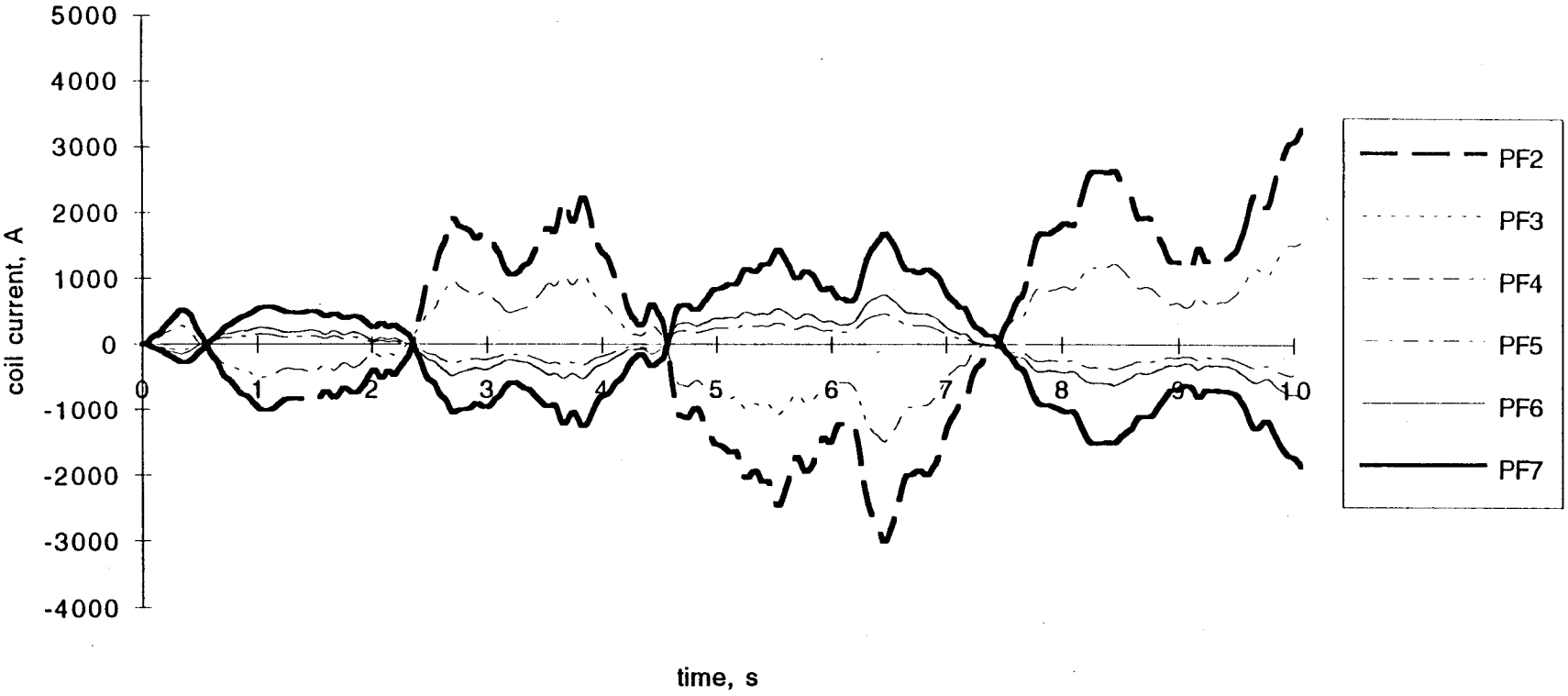

Fig. 3.1-2.a Vertical control coils current simulation, t_r=3 s, Opt.#1b

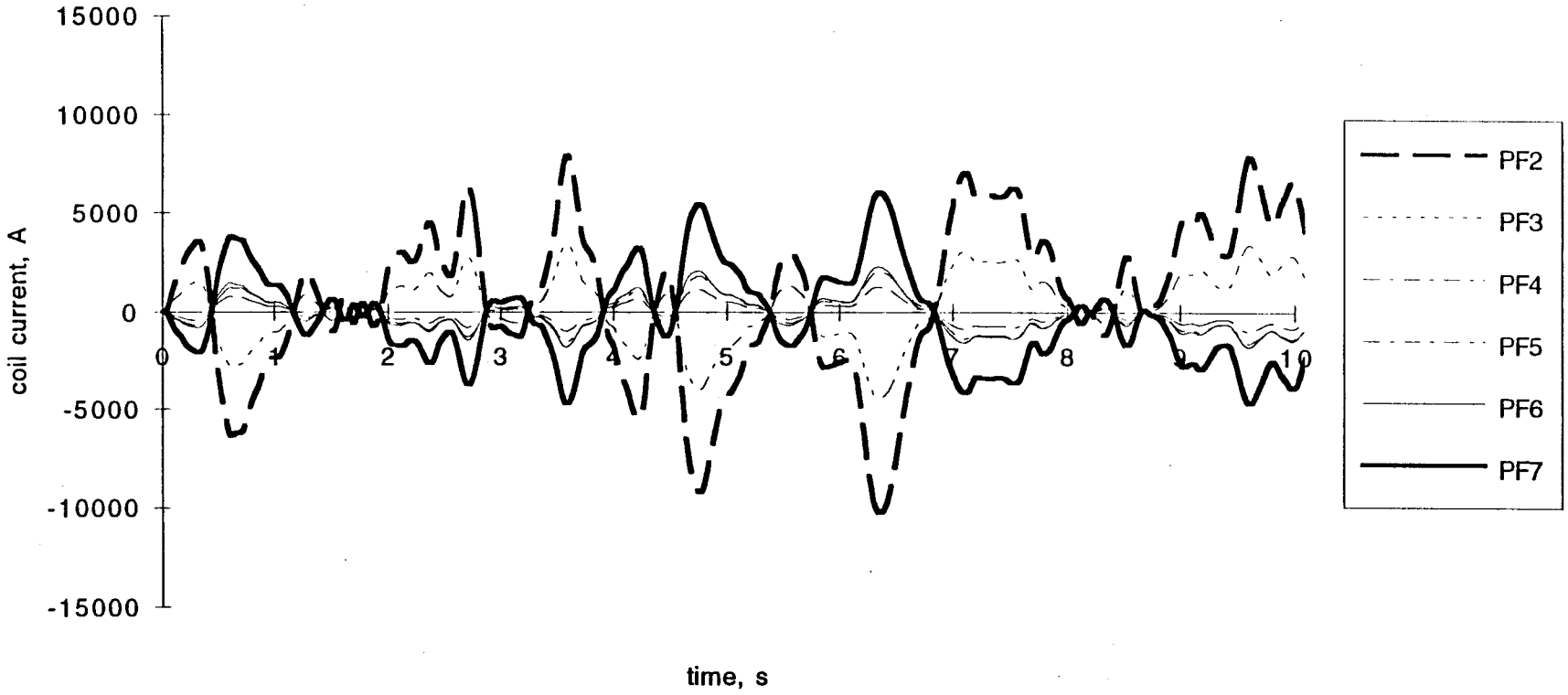

Fig. 3.1-2.b Vertical control coils current simulation, t_r=1 s, Opt.#1b

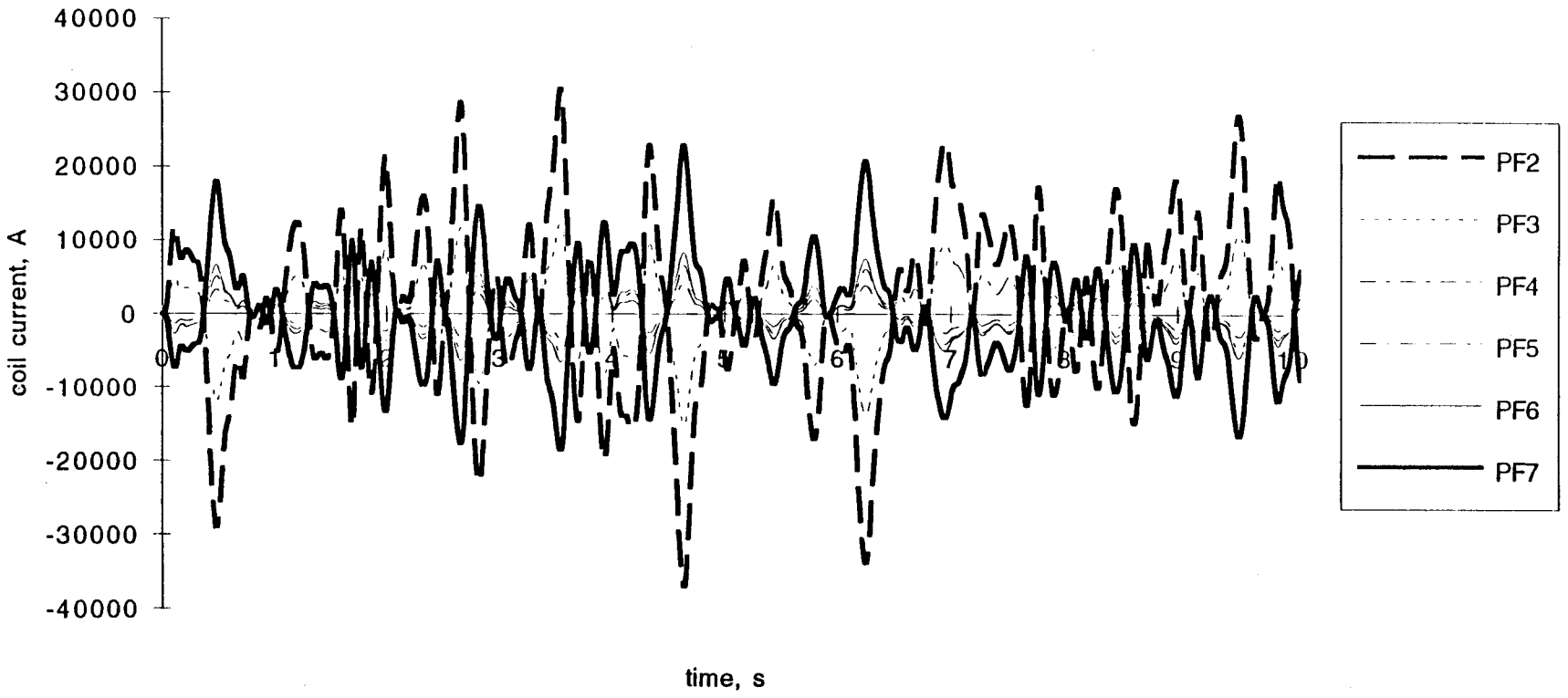

Fig. 3.1-2.c Vertical control coils current simulation, t_r=1/3 s, Opt.#1b

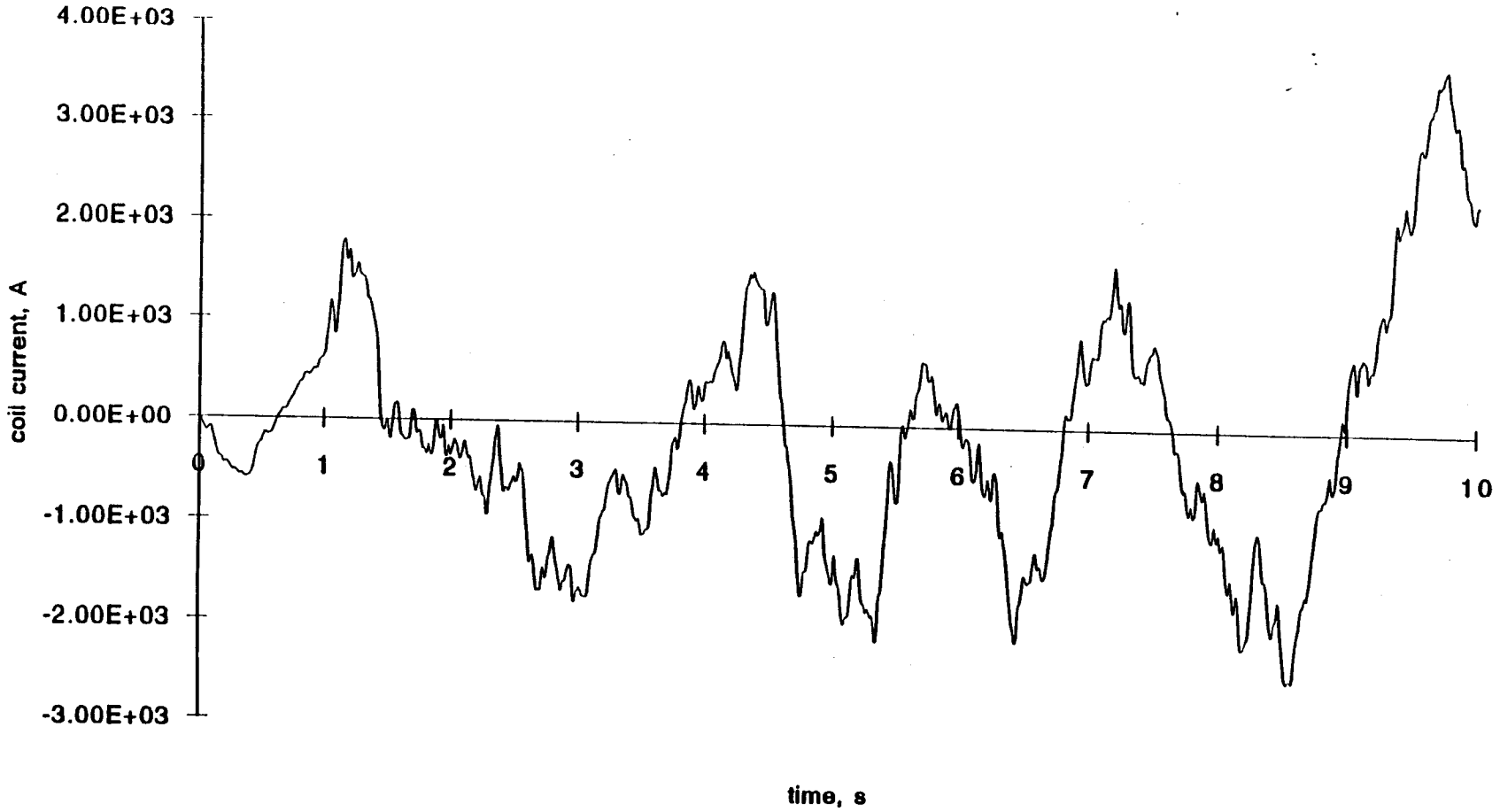

Fig. 3.1-3.a Vertical control coils current simulation, t_r=3 s, Opt.#2

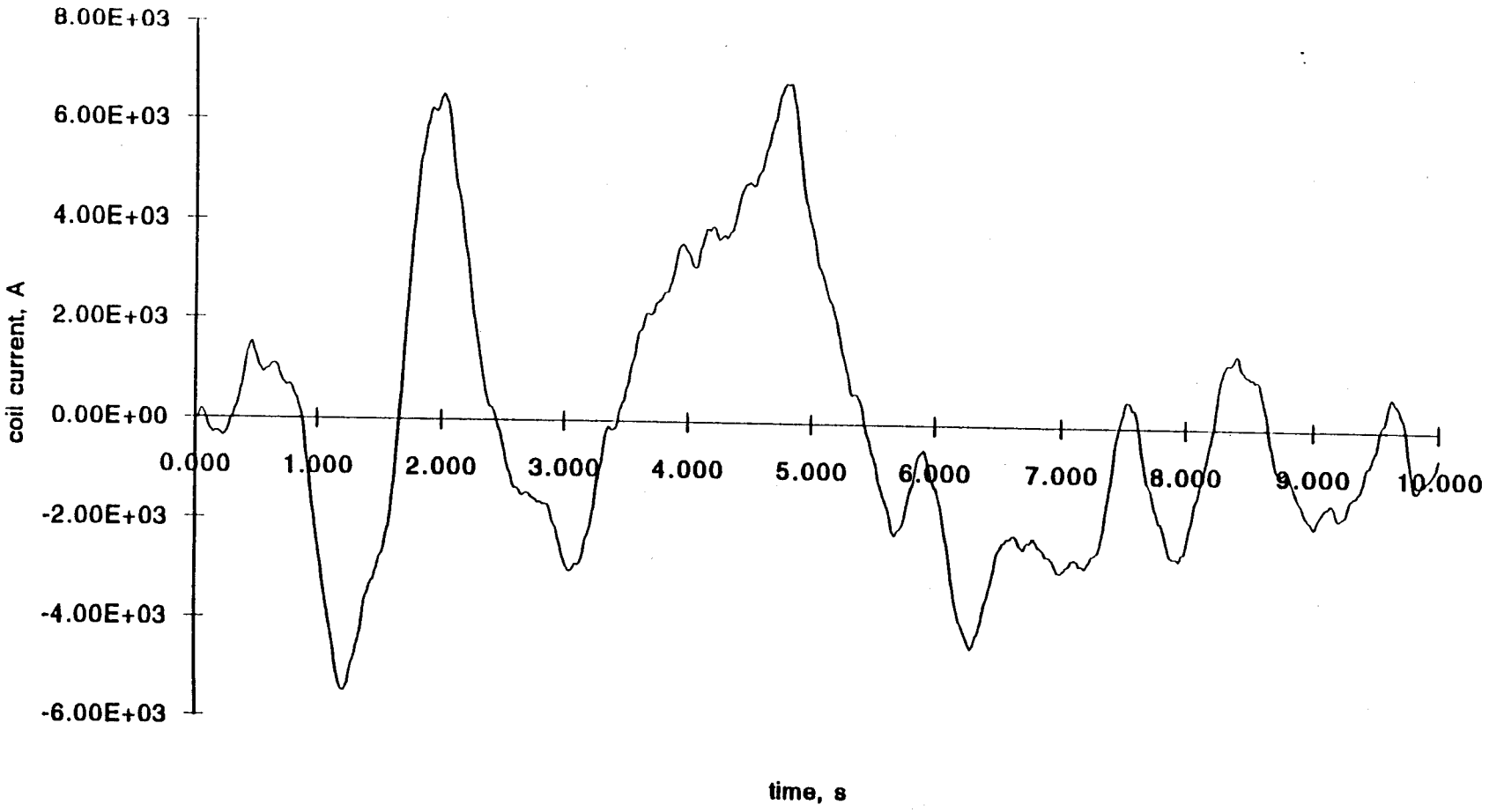

Fig. 3.1-3.b Vertical control coils current simulation, t_r=1 s, Opt.#2

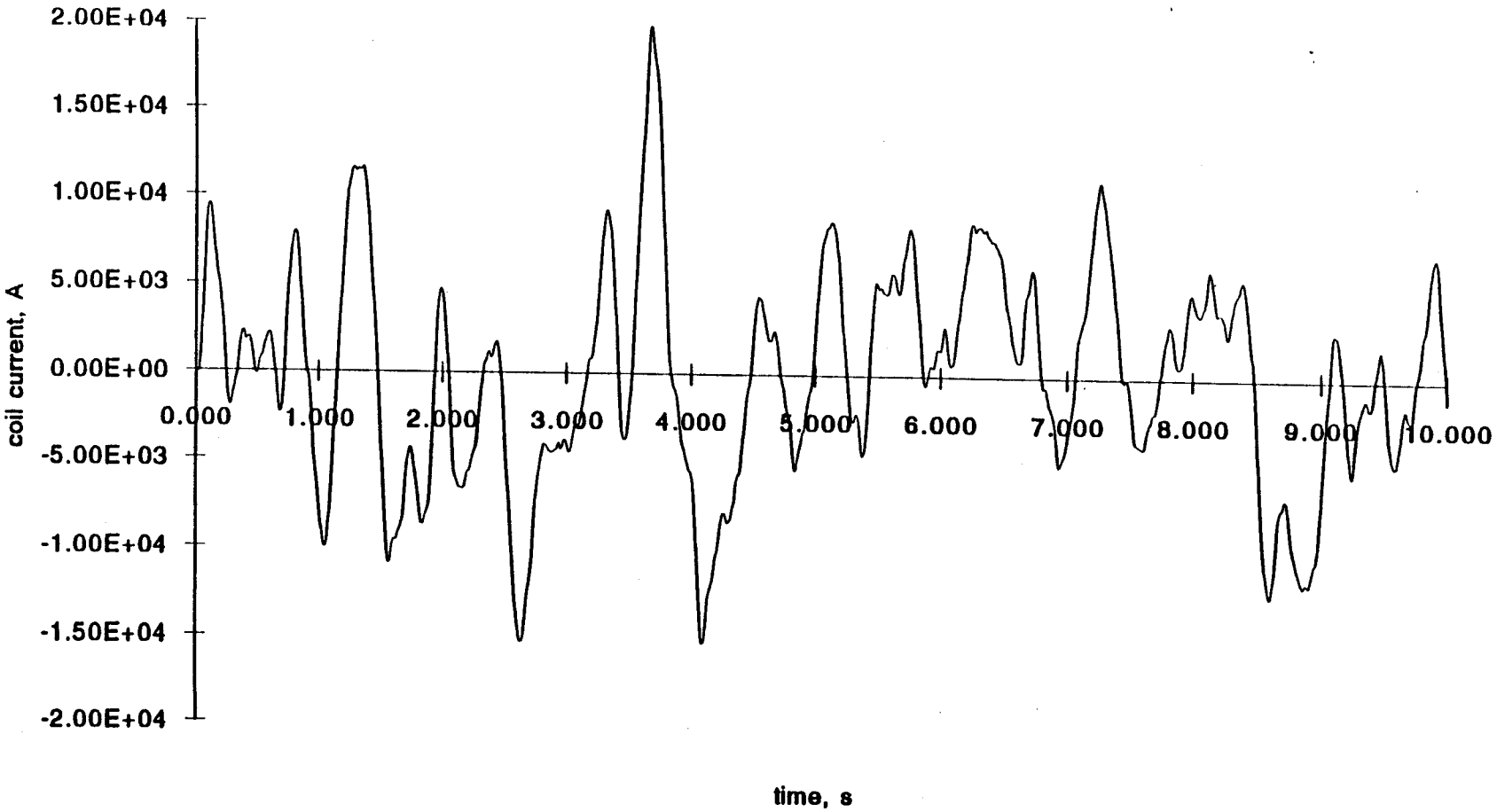

Fig. 3.1-3.c Vertical control coils current simulation, t_r=1/3 s, Opt.#2

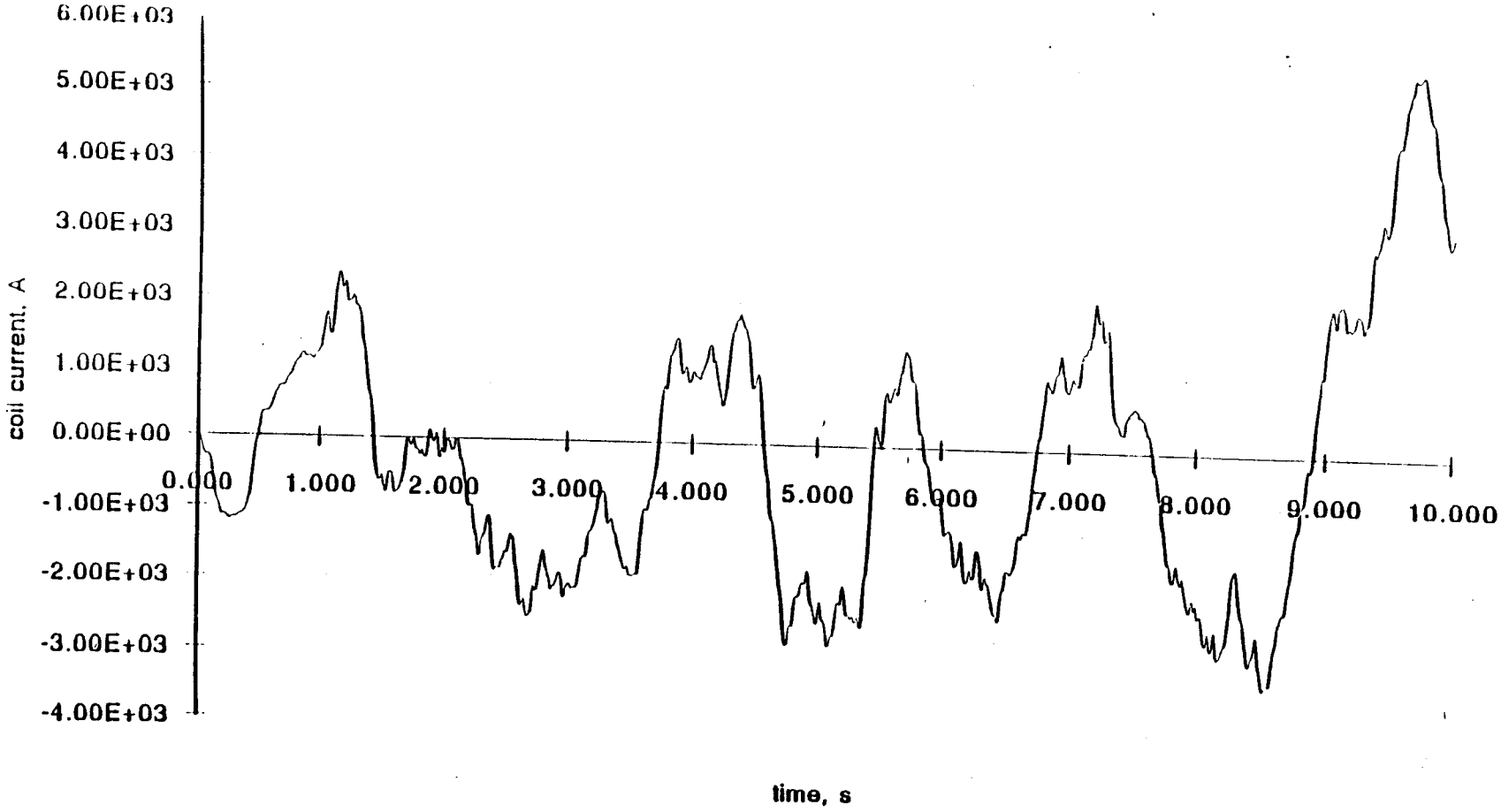

Fig. 3.1-4.a Vertical control coils current simulation, t_r=3 s, Opt.#3

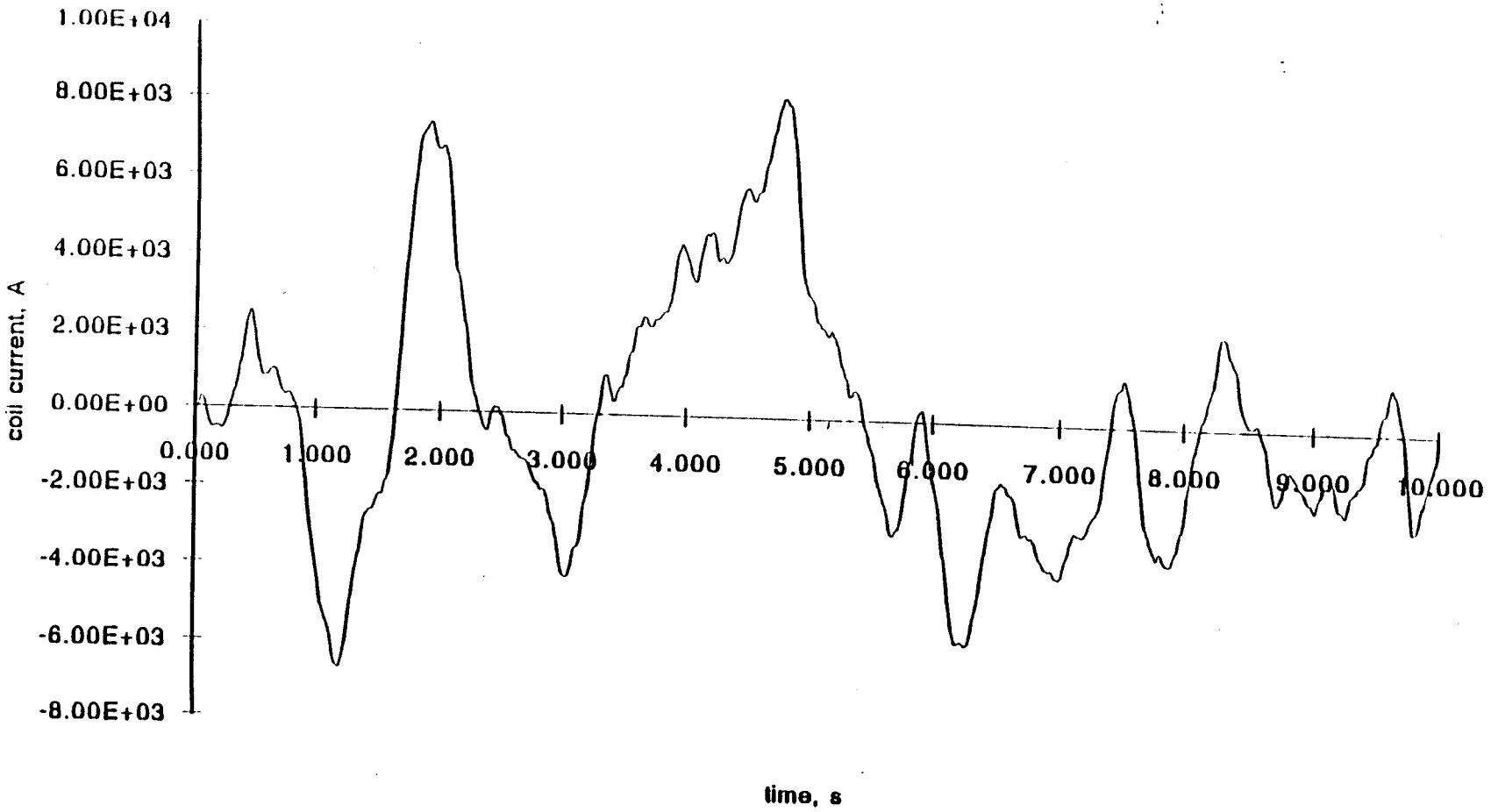

Fig. 3.1-4.b Vertical control coils current simulation, t_r=1 s, Opt.#3

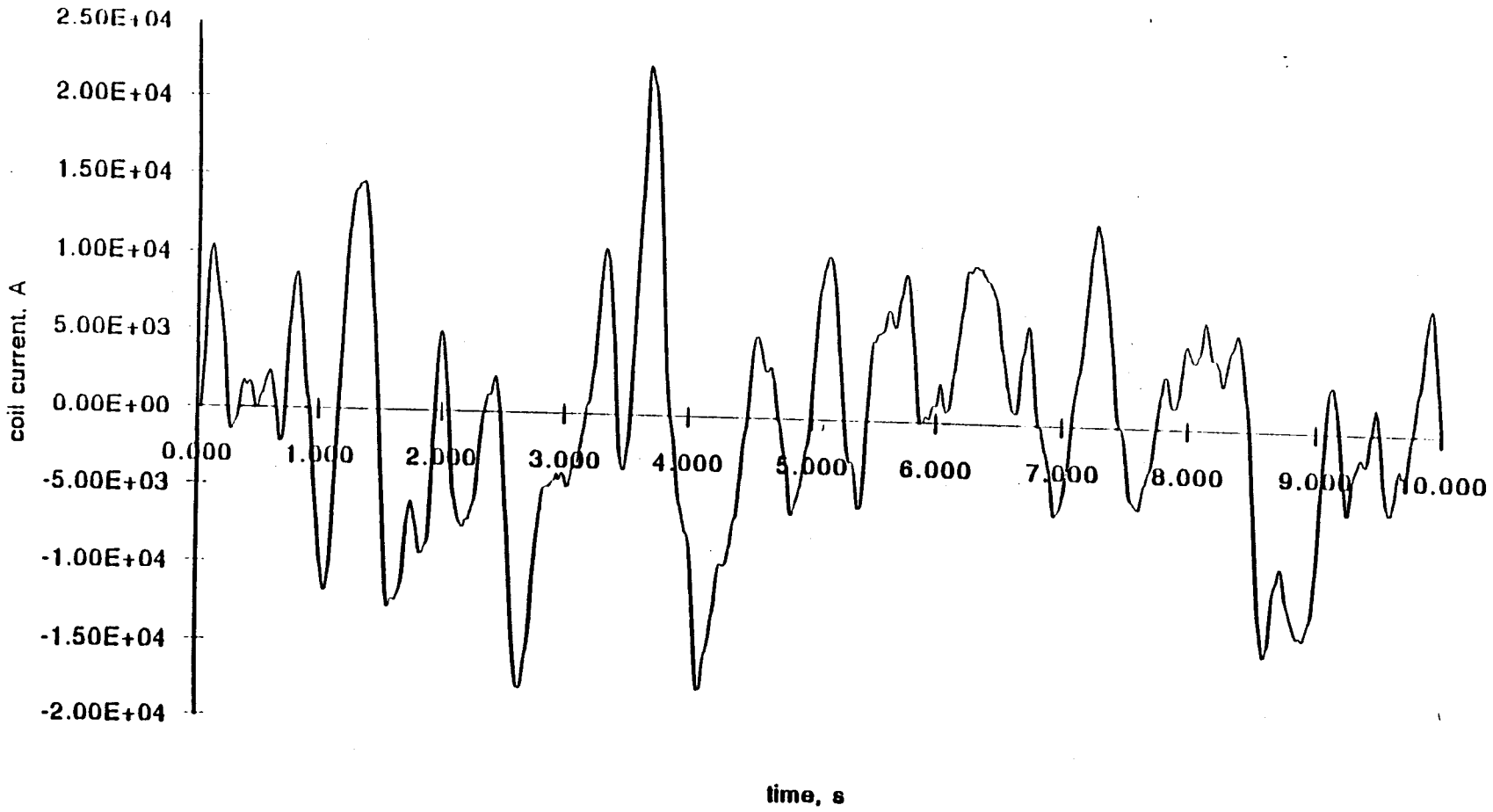

Fig. 3.1-4.c Vertical control coils current simulation, t_r=1/3 s, Opt.#3

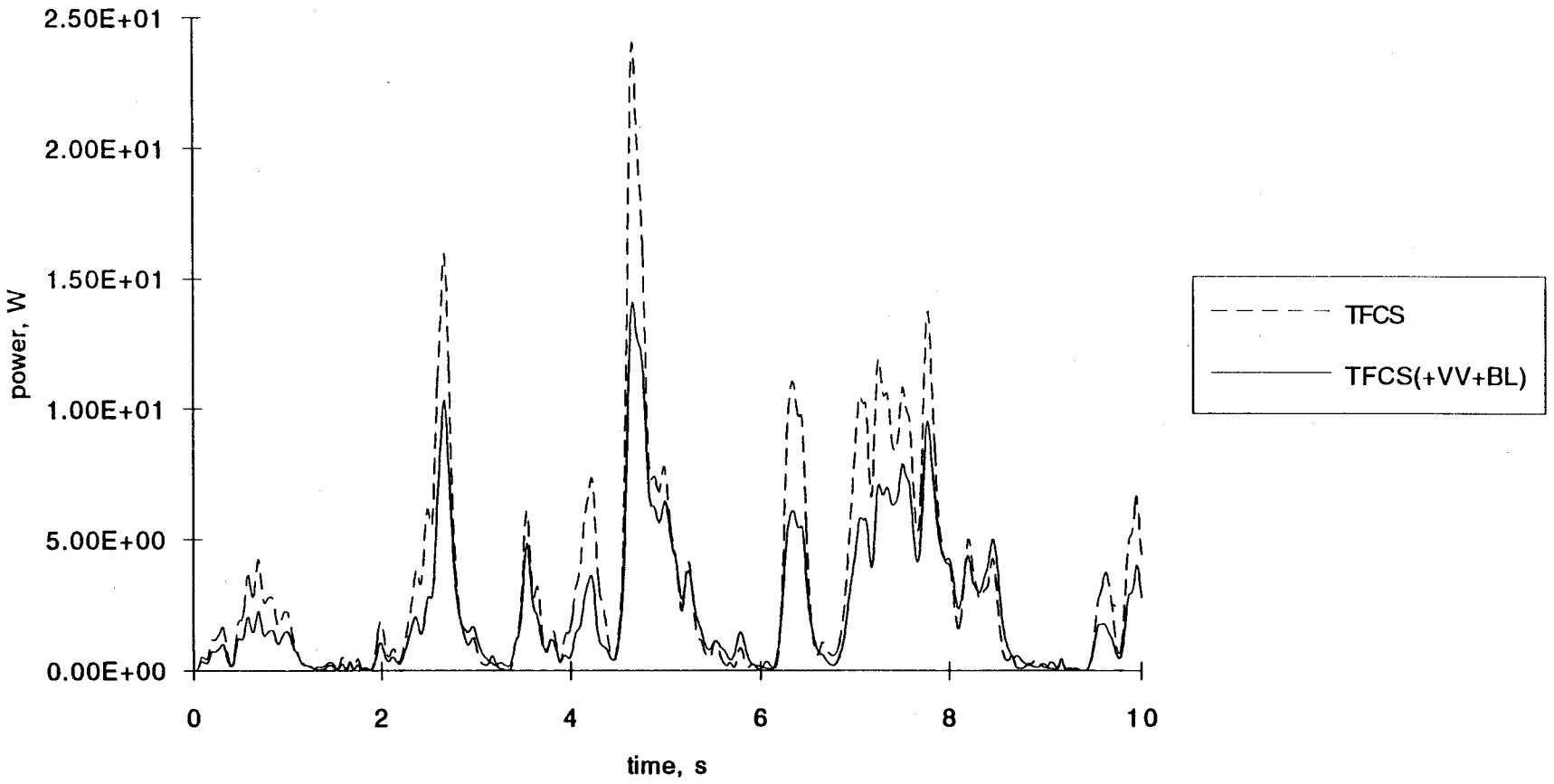

Fig. 3.2-1.a Power deposition in the TF cold structure, t_r=3 s, Opt.#1a

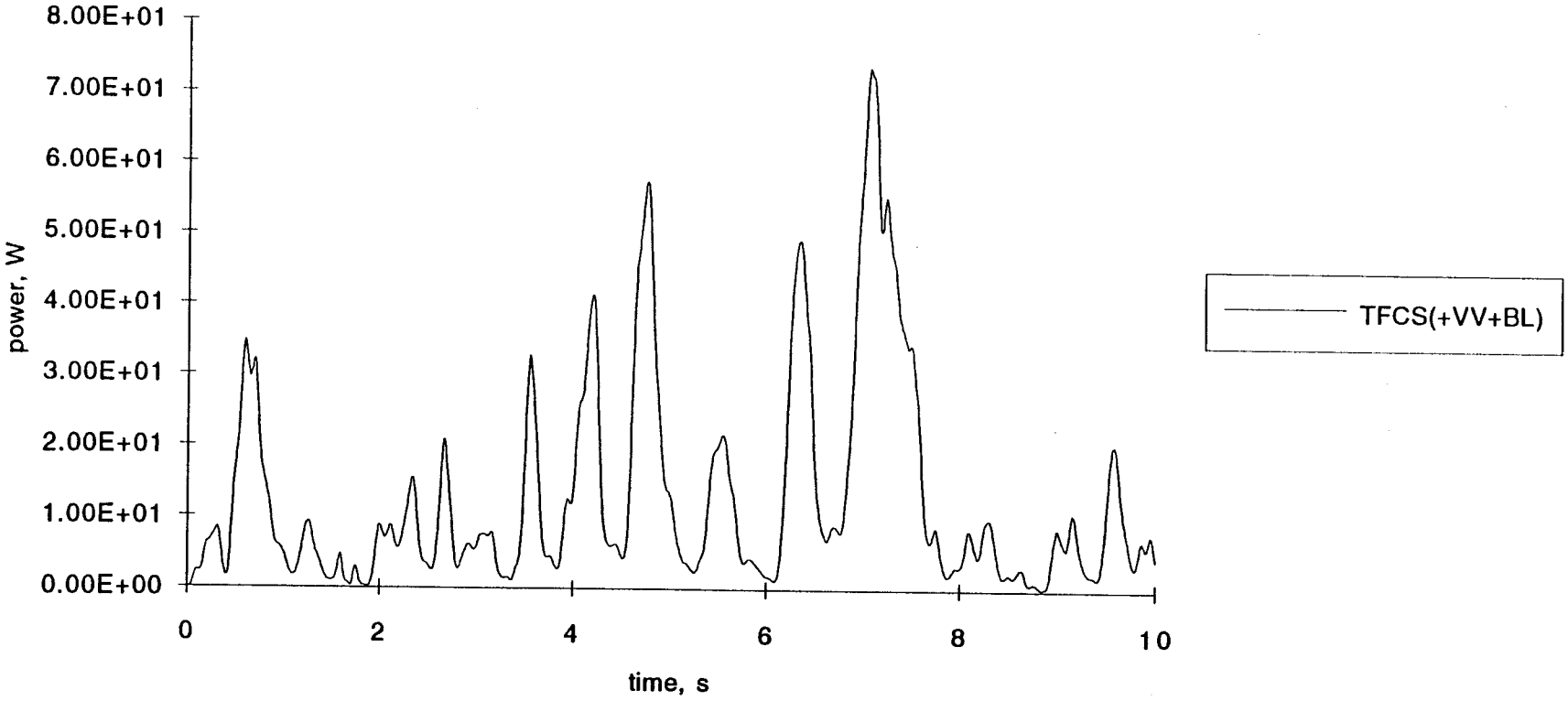

Fig. 3.2-1.b Power deposition in the TF cold structure, t_r=1 s, Opt.#1a

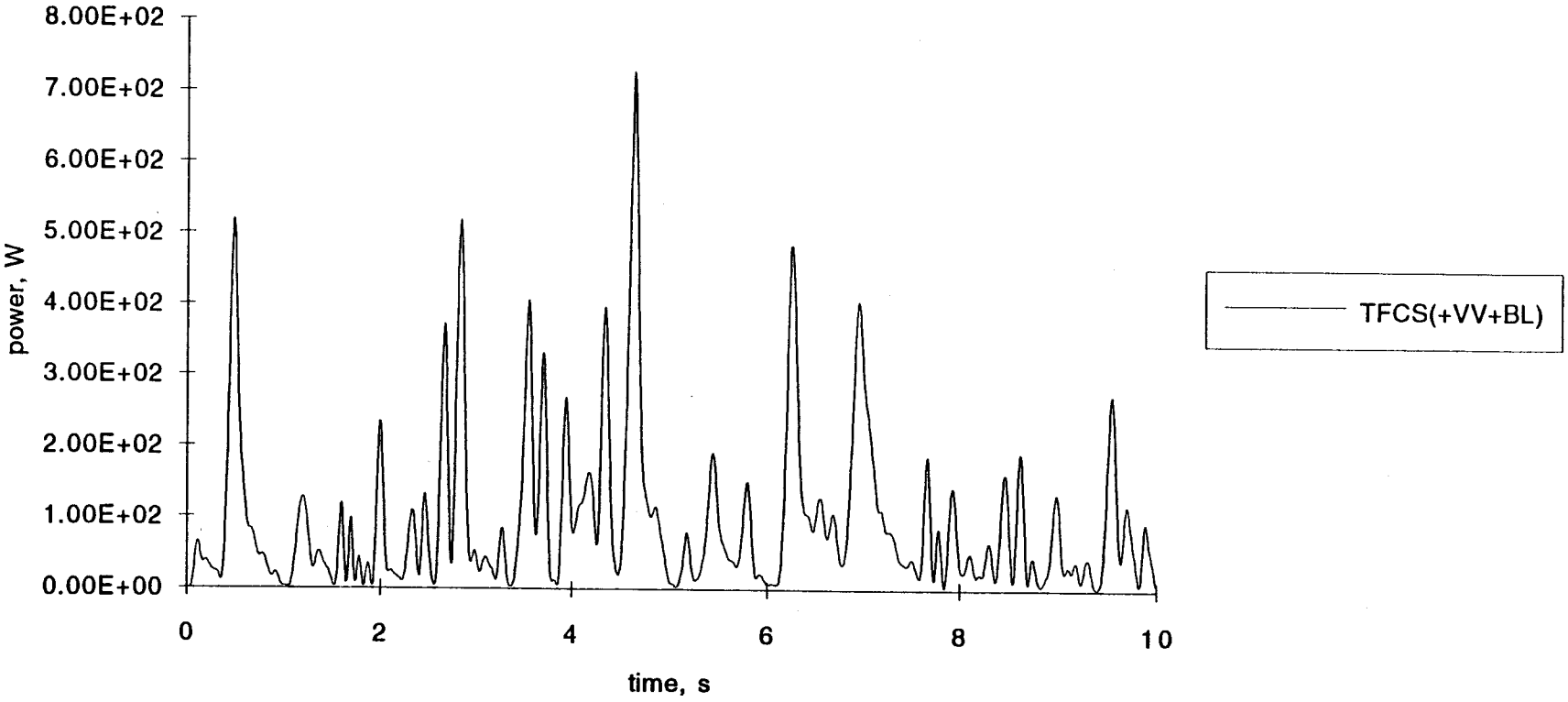

Fig. 3.2-1.c Power deposition in the TF cold structure, t_r=1/3 s, Opt.#1a

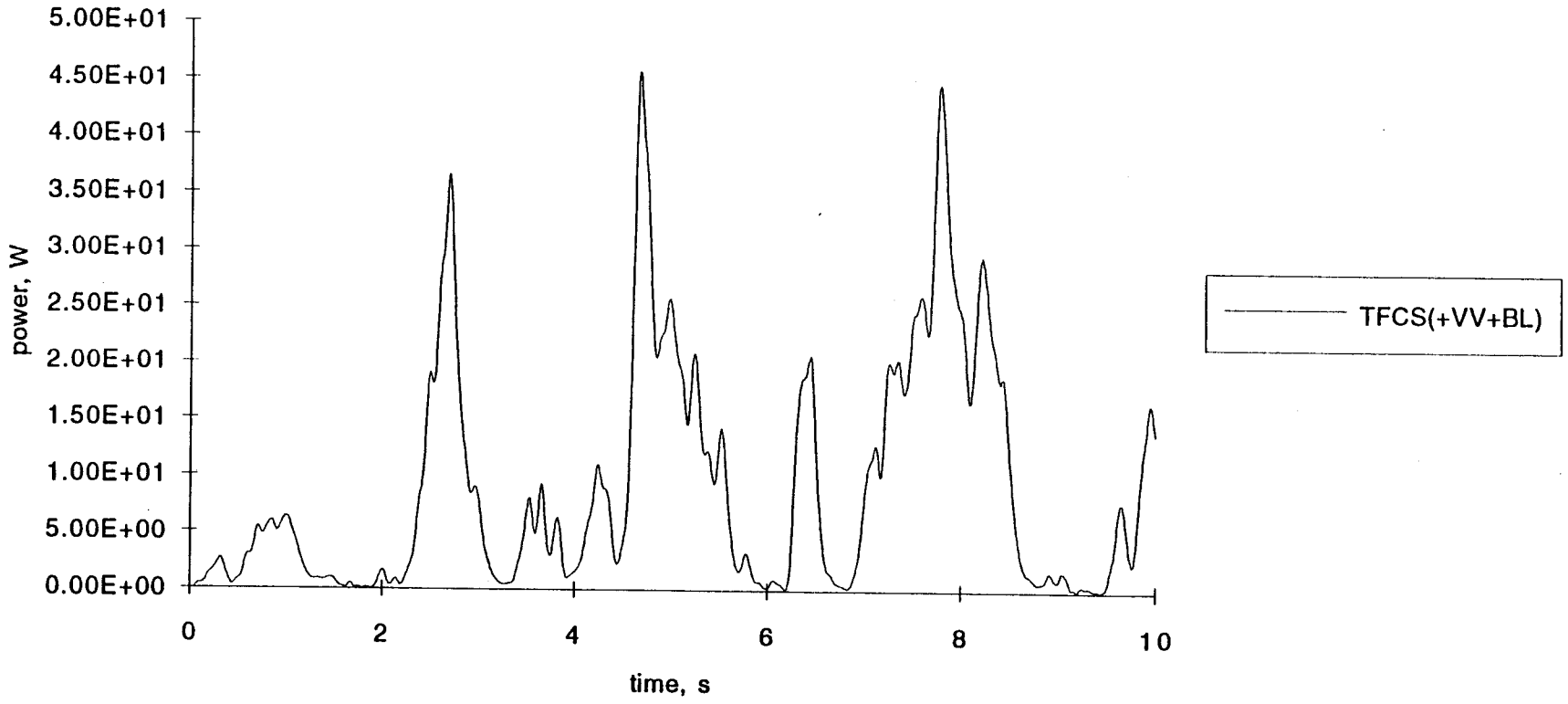

Fig. 3.2-2.a Power deposition in the TF cold structure, t_r=3 s, Opt.#1b

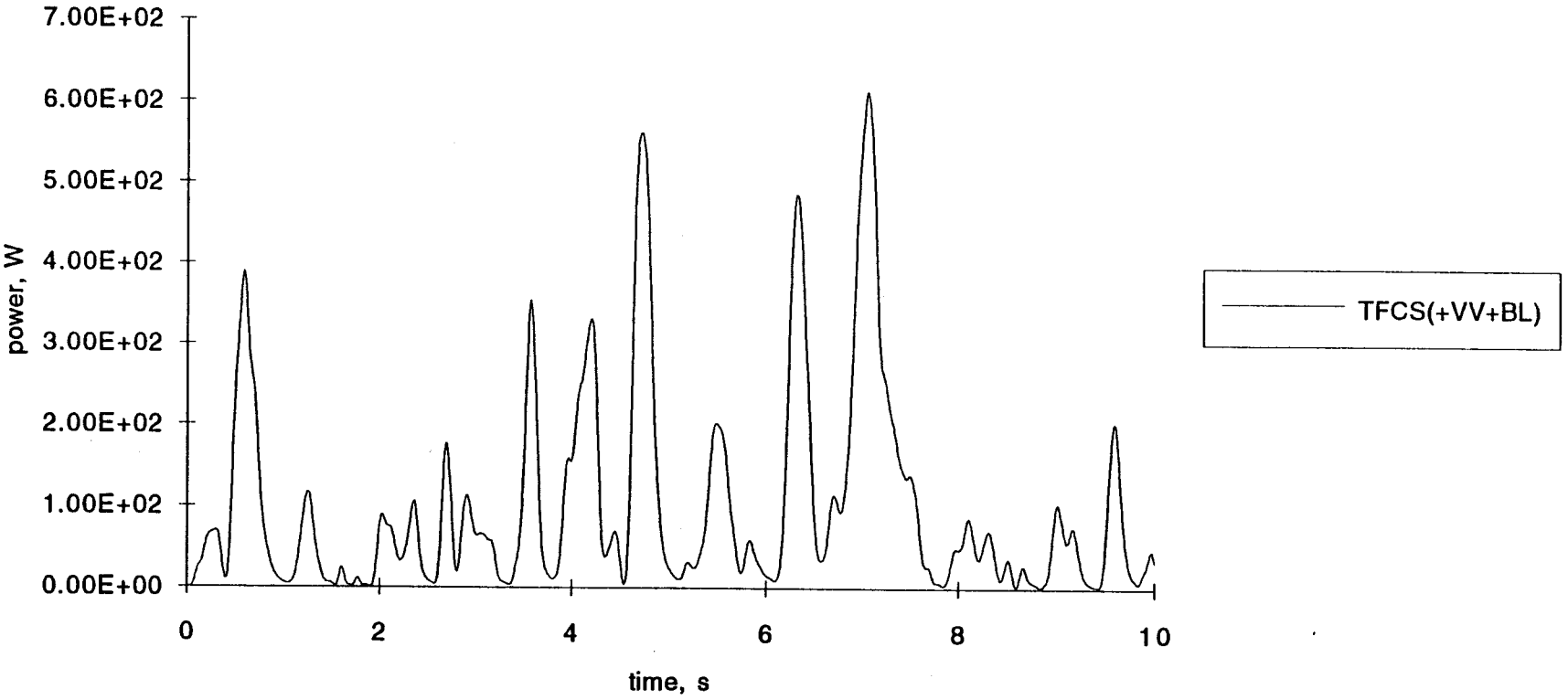

Fig. 3.2-2.b Power deposition in the TF cold structure, t_r=1 s, Opt.#1b

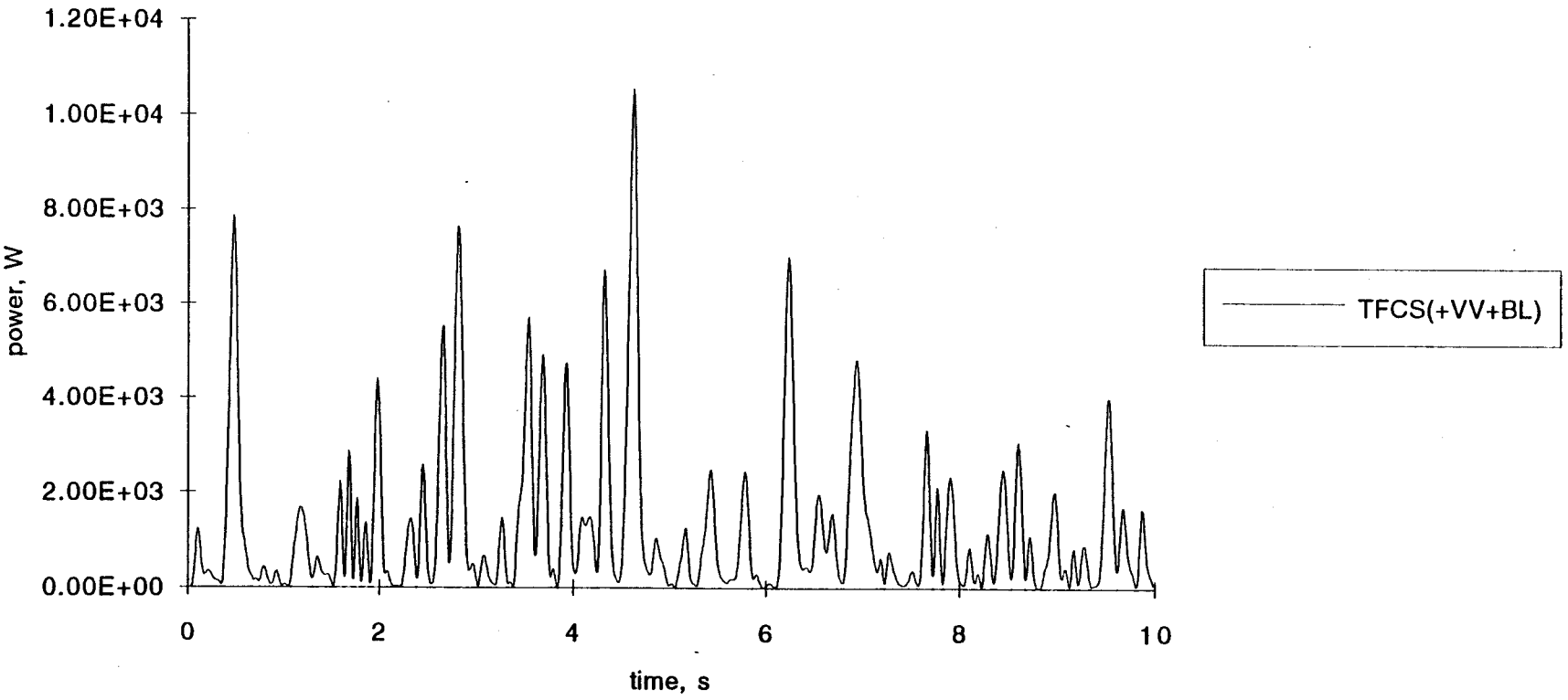

Fig. 3.2-2.c Power deposition in the TF cold structure, t_r=1/3 s, Opt.#1b

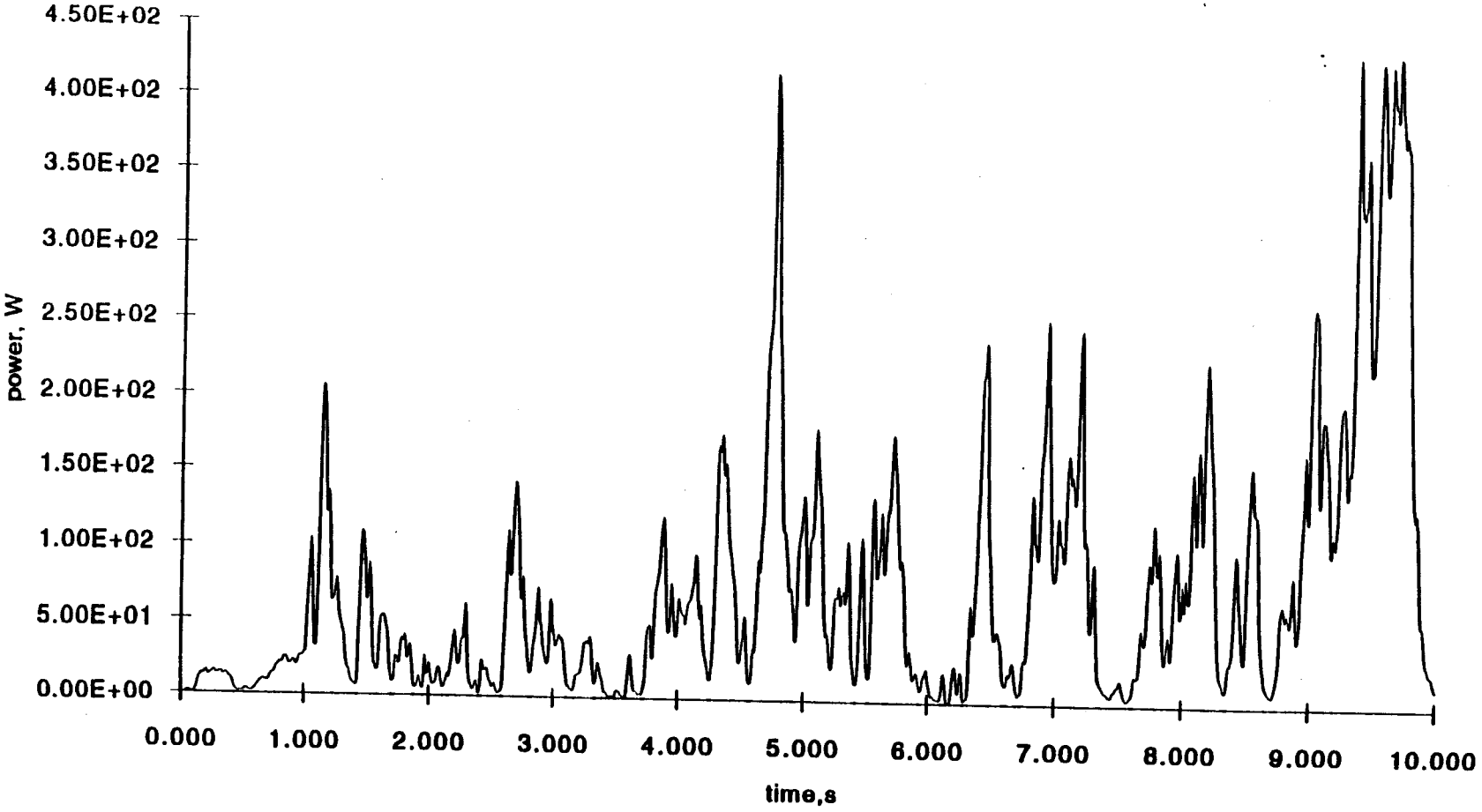

Fig. 3.2-3.a Power deposition in the TF cold structure, t_r=3 s, Opt.#2

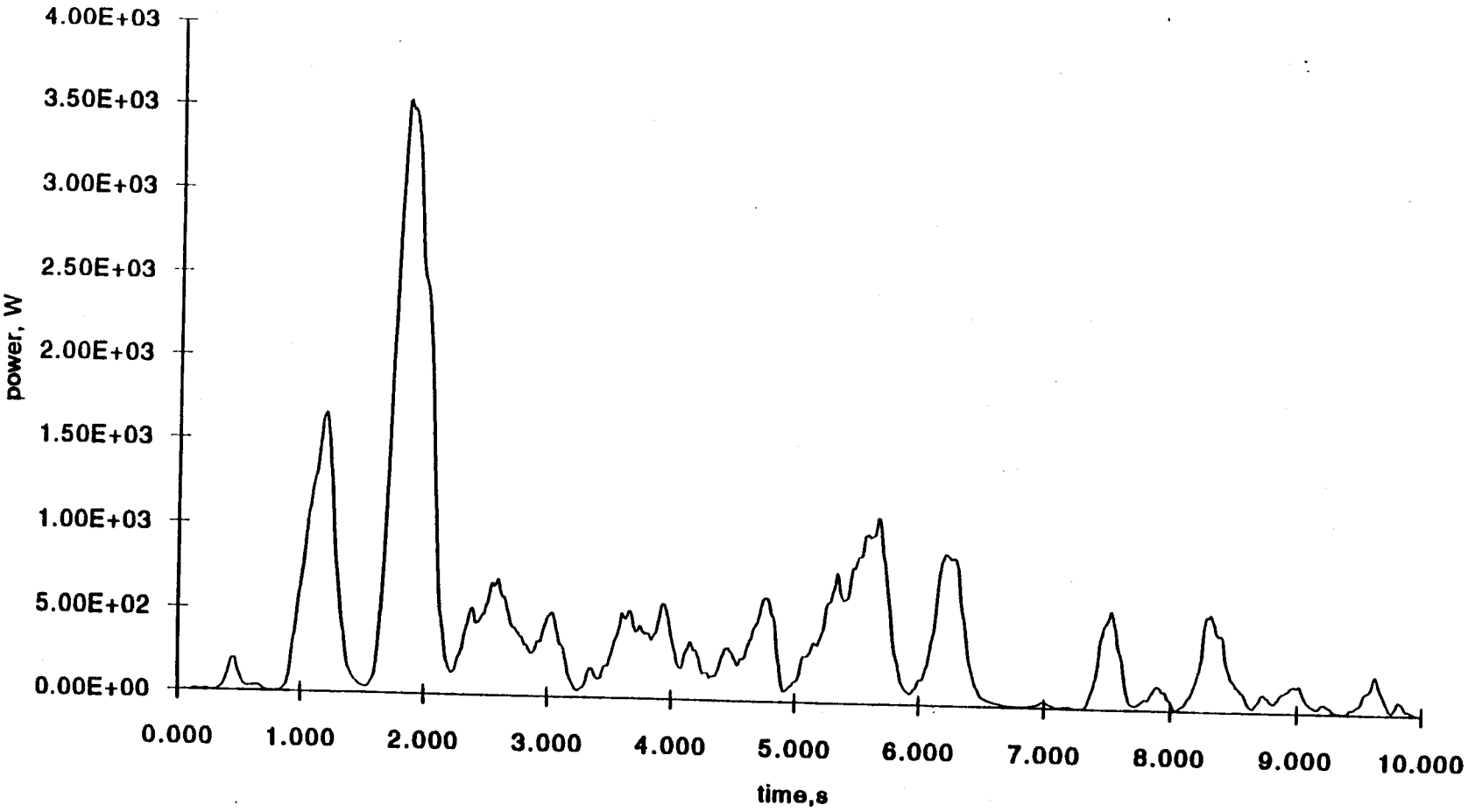

Fig. 3.2-3.b Power deposition in the TF cold structure, t_r=1 s, Opt.#2

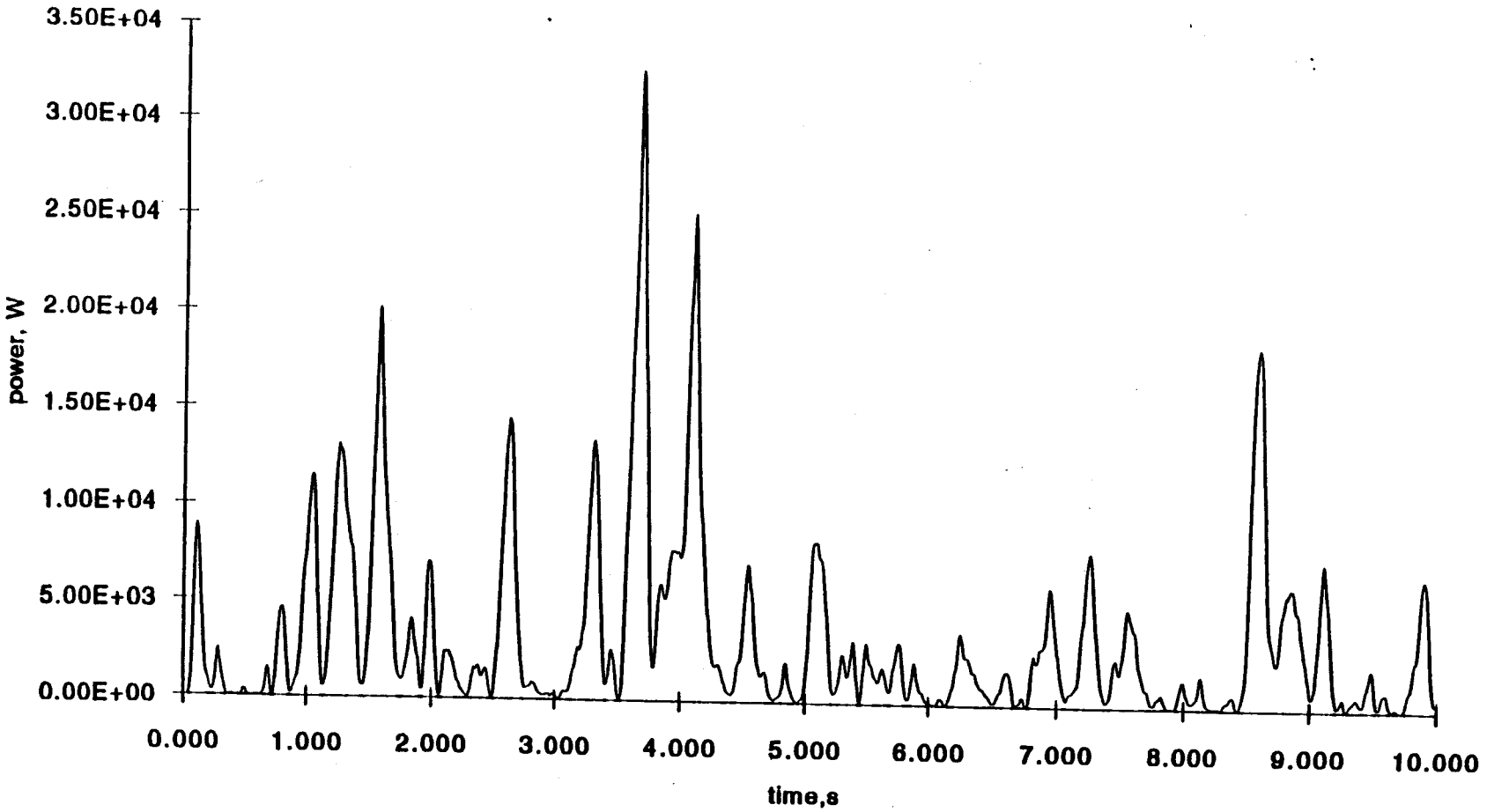

Fig. 3.2-3.c Power deposition in the TF cold structure, t_r=1/3 s, Opt.#2

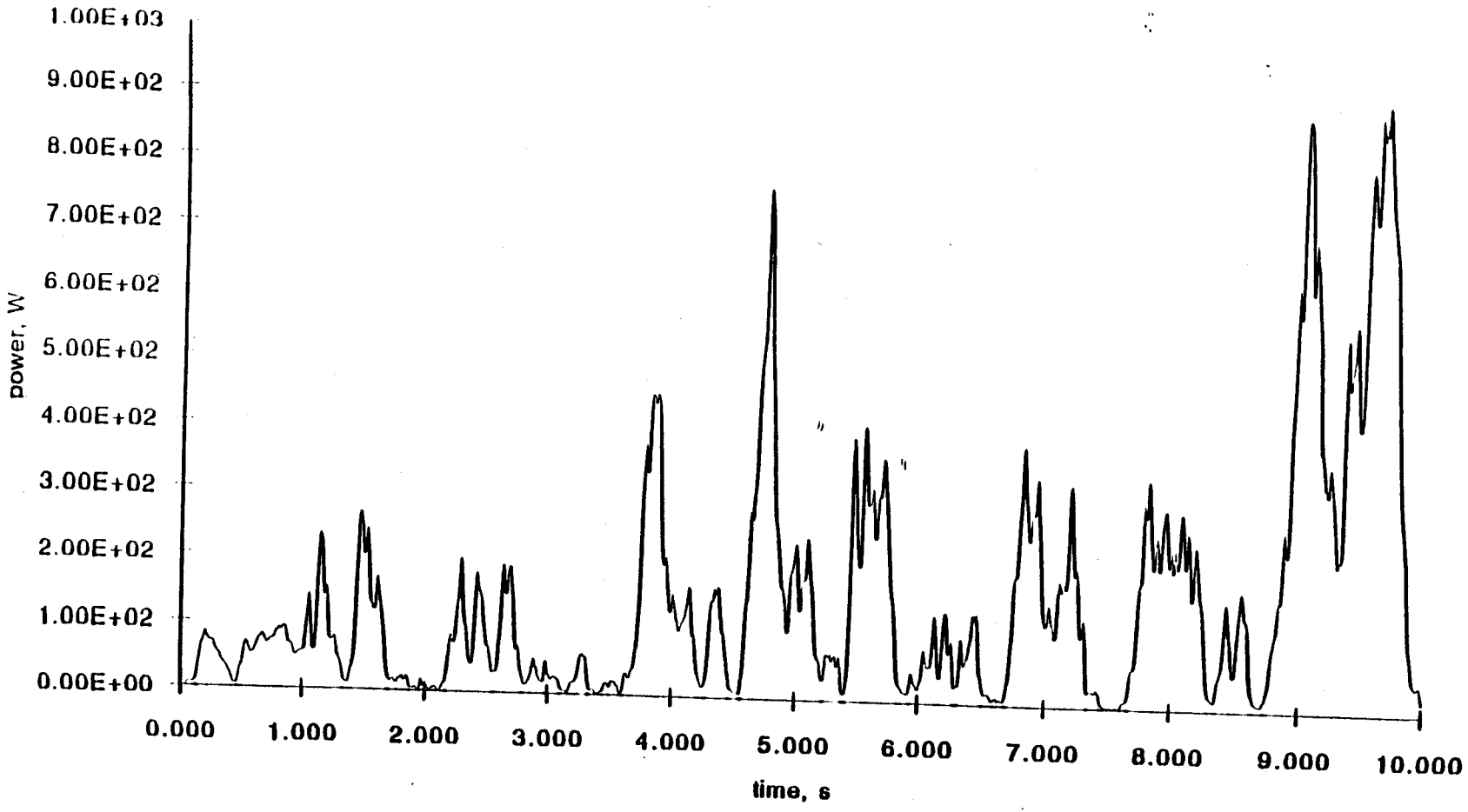

Fig. 3.2-4.a Power deposition in the TF cold structure, t_r=3 s, Opt.#3

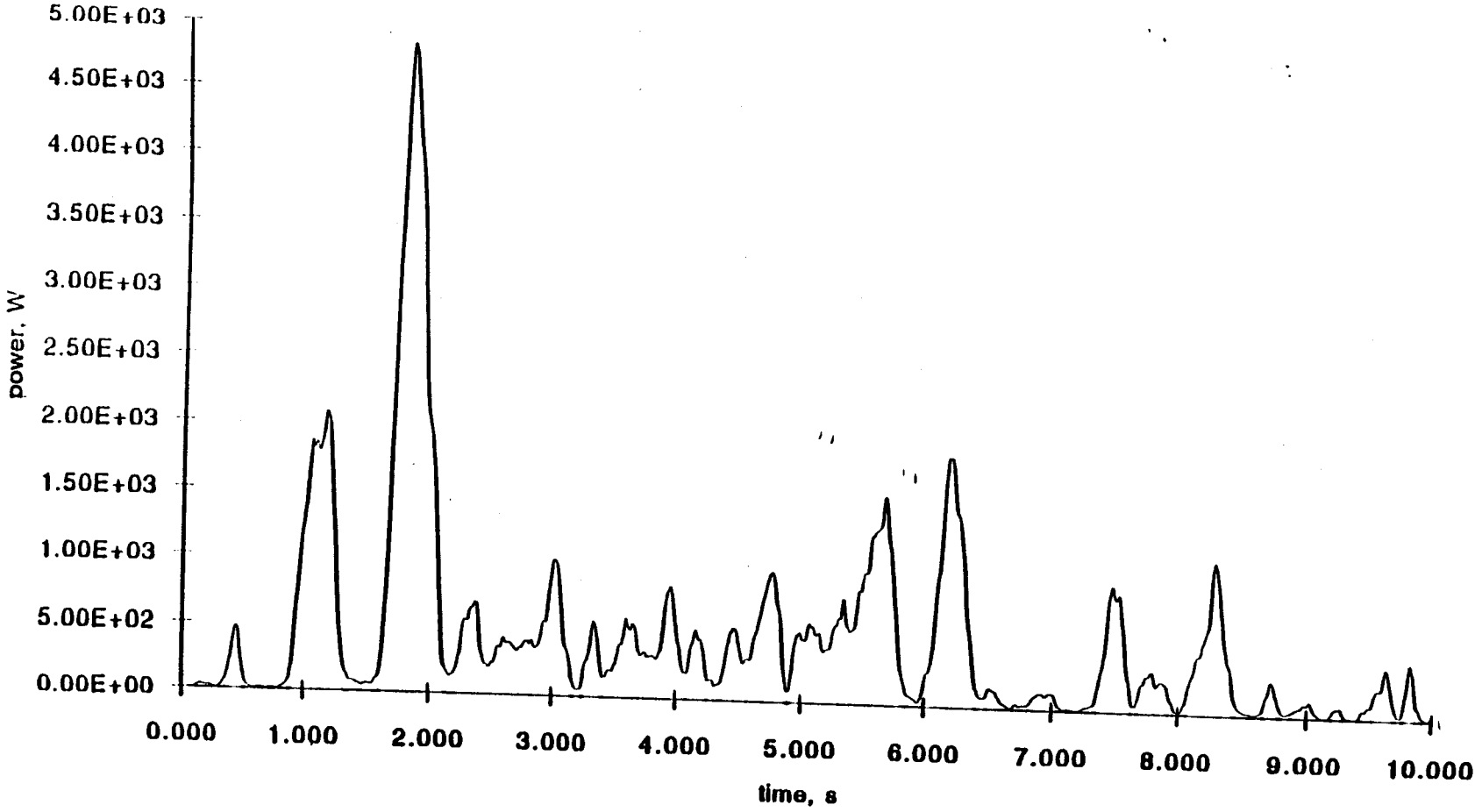

Fig. 3.2-4.b Power deposition in the TF cold structure, t_r=1 s, Opt.#3

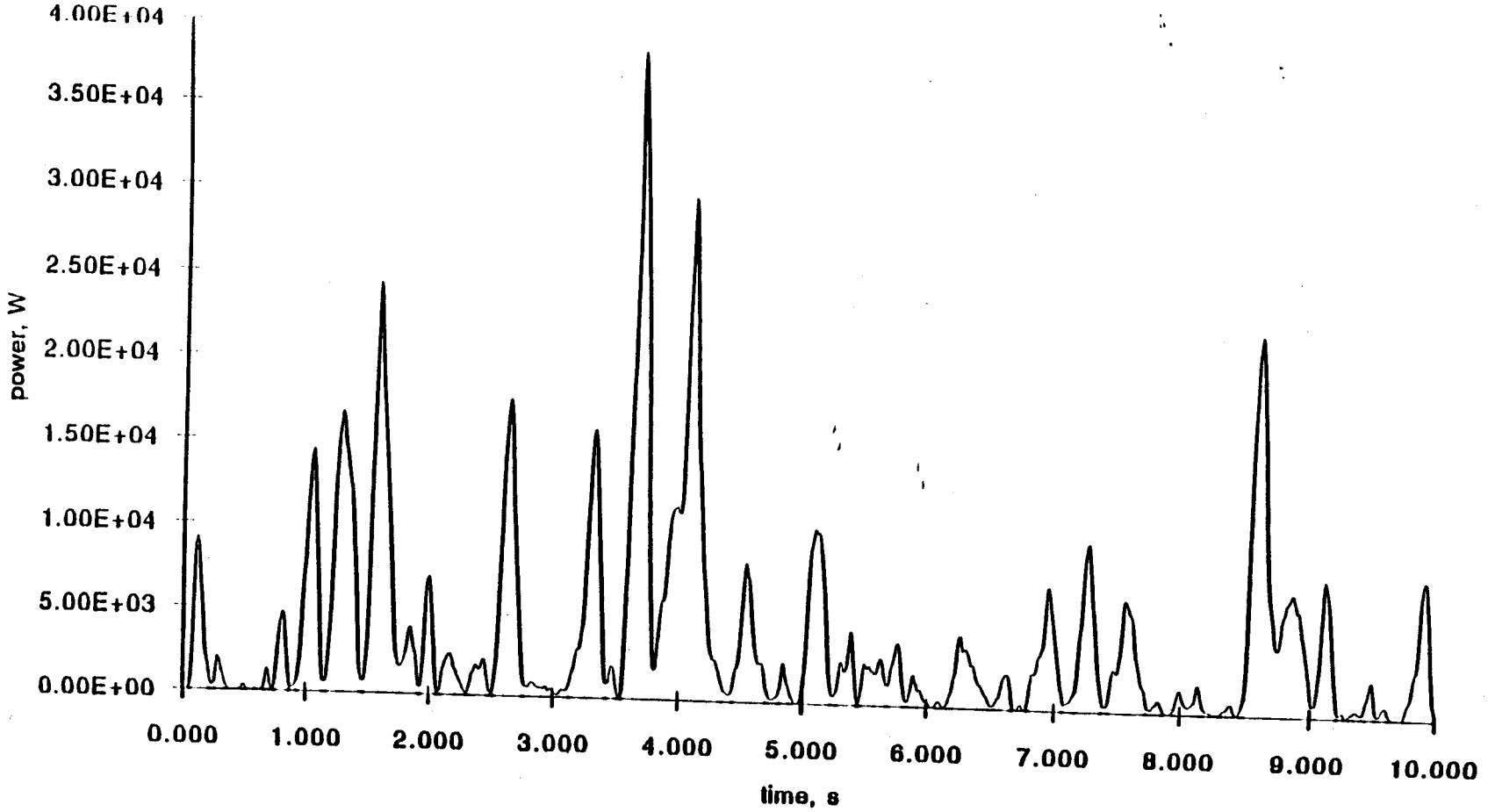

Fig. 3.2-4.c Power deposition in the TF cold structure, t_r=1/3 s, Opt.#3

only the TFCS (dashed line). The results show that the effect of shielding the TFCS with the vacuum vessel and the blanket is significant in this case, accounting for about 40% of the power deposited in the TFCS. It can be explained by the fact that in these cases the magnetic field is driven primarily by coils PF2 and PF7 which are located near the top and the bottom of the vacuum vessel, where, as is shown in Figs. 3.2-5.a and 3.2-5.b, the highest density of eddy currents occurs. The same is applicable to Option #1b. The eddy current patterns shown in Figures 3.2-5.a and 3.2-5.b are obtained for Option #1a and are typical for Option #1b. Figure 3.2-6 shows the pattern of the eddy currents in the TFCS for Option #3, which is typical also for Option #2.

The average power dissipation over the 10-second time period modeled is:

t_r	Option #1a	Option #1b	Option #2	Option #3
3 s	3.32 W	9.08 W	76 W	160 W
1 s	13.0 W	101 W	380 W	490 W
1/3 s	97.1 W	1242 W	3380 W	4190 W

The dramatic drop in power dissipation in the TFCS in Option #1a is primarily due to the fact that in this case currents in coils PF3 and PF5 driven by the flux caused by PF2 and PF7 provide a shielding effect to the TFCS. Another reason is that in Option #1a the driving coils PF2 and PF7 are much farther from the TFCS than coils used in Options #1b, #2, or #3.

4.0 Joule Heating of the ITER TF Cold Structure due to ELMs

Sets of four sequential ELMs, as well as isolated ELMs have been studied for various sets of active PF coils. The results showed that the lowest average power dissipation in the TF cold structure occurs when PF2 and PF7 are active, and all other PF coils are passive.

4.1 Current versus Time Scenarios

The current versus time laws were defined as follows.

Case ELM2 :

ELM2 is defined by [8]. Coils PF2 and PF7 are active, coils PF1 and PF3-PF6 are passive and are driven by a condition of constant flux. The ampere-turns versus time scenario is shown in Fig. 4.1-1. Four ELMs were modeled over a time interval of 4 seconds.

Case ELM6 :

ELM6 is defined by [9]. Coils PF2-PF7 are active, coil PF1 is passive and carries only the current induced under the condition of constant flux. The

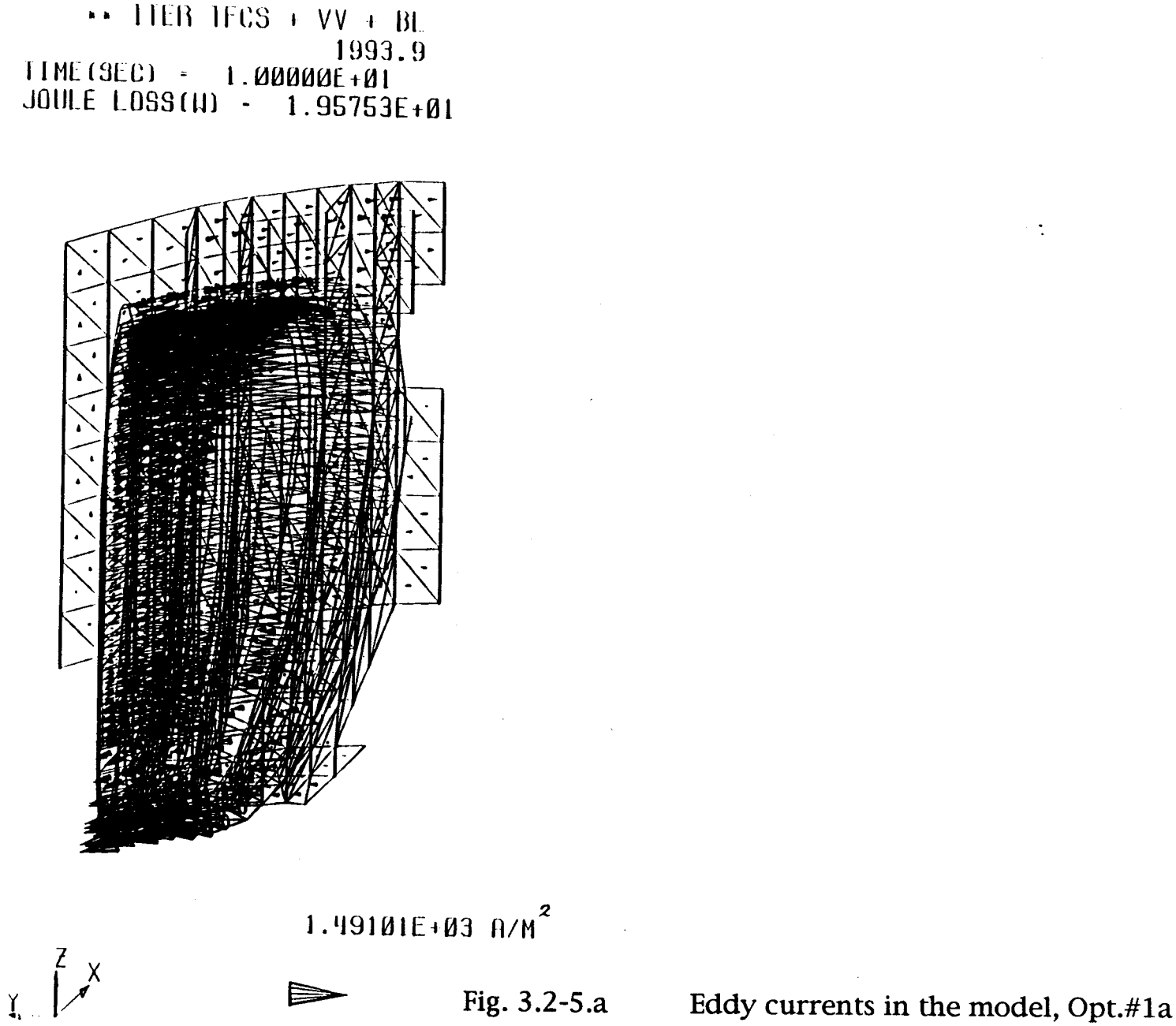

Fig. 3.2-5.a Eddy currents in the model, Opt.#1a

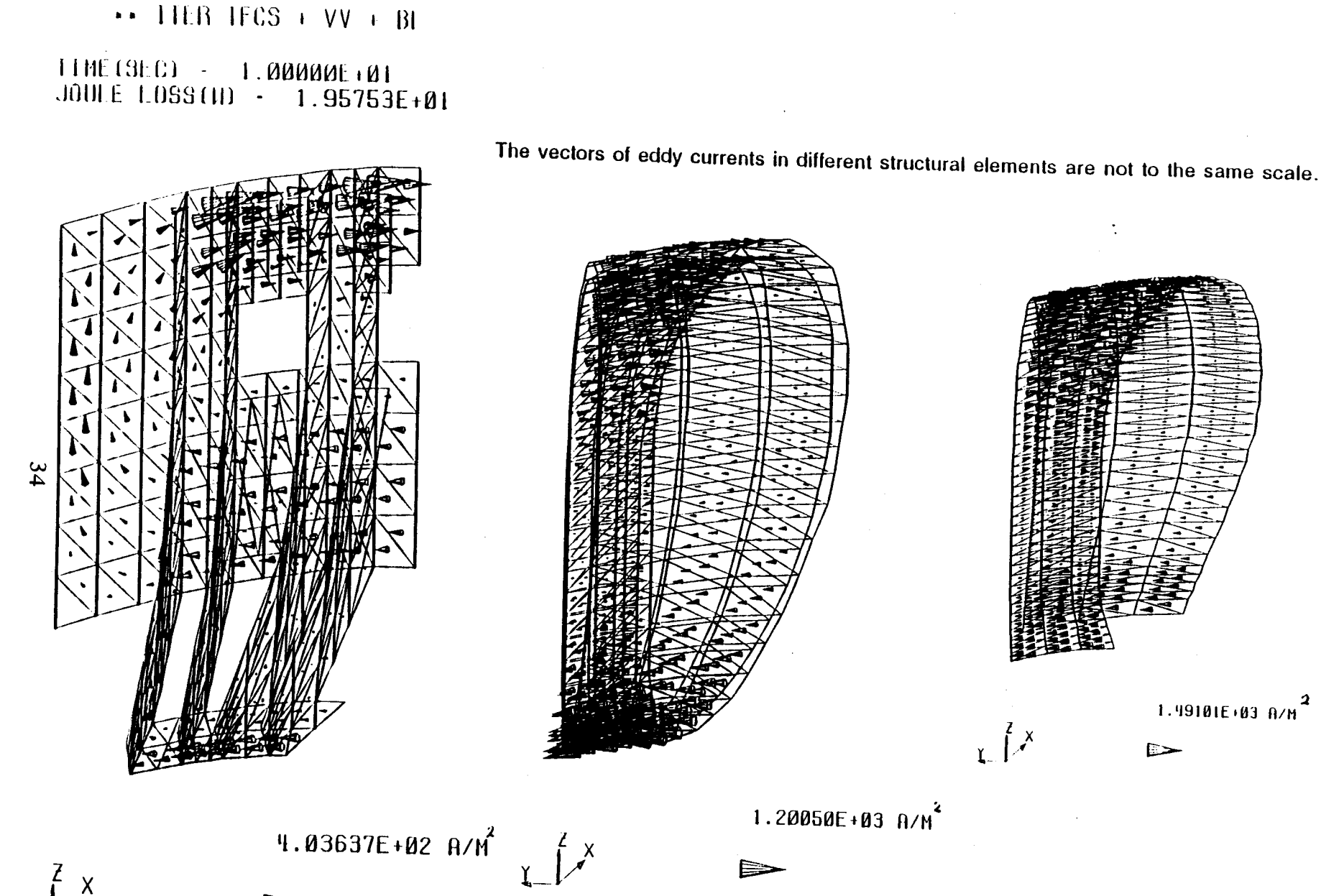

Fig. 3.2-5.b Eddy currents in the structural elements, Opt.#1a

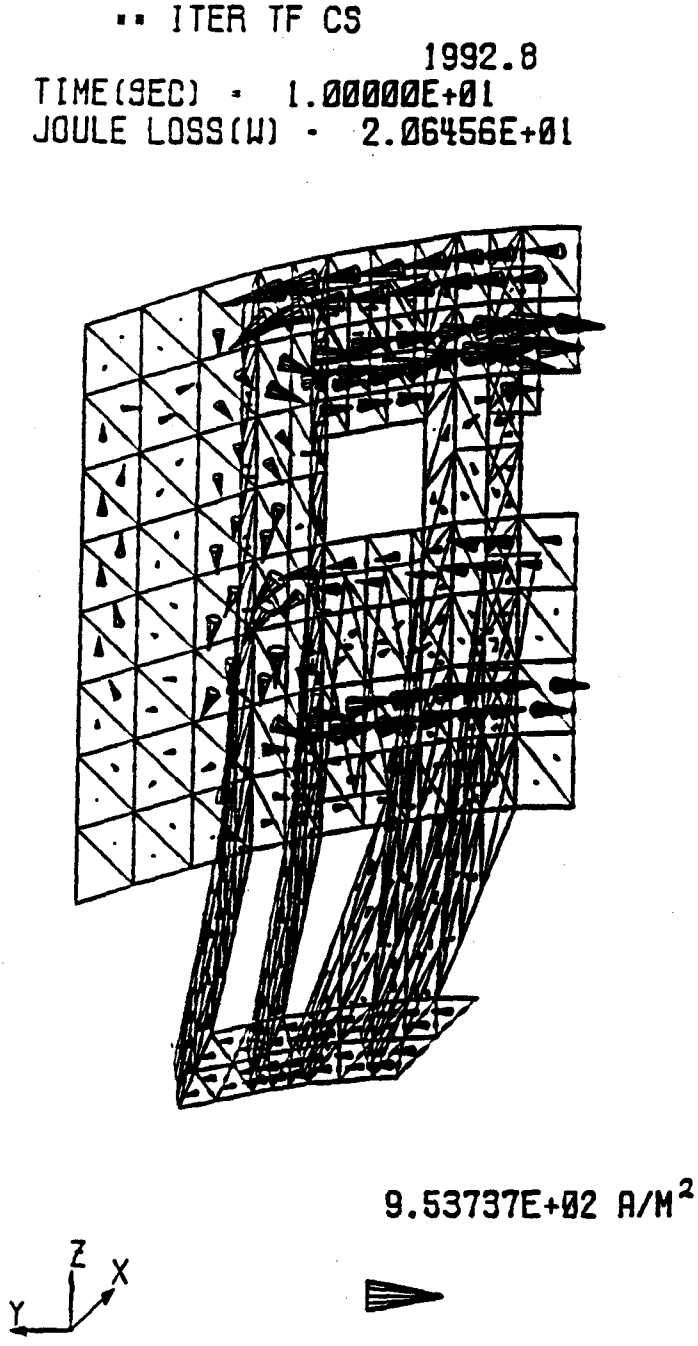

Fig. 3.2-6 Eddy currents in the model, Opt.#3

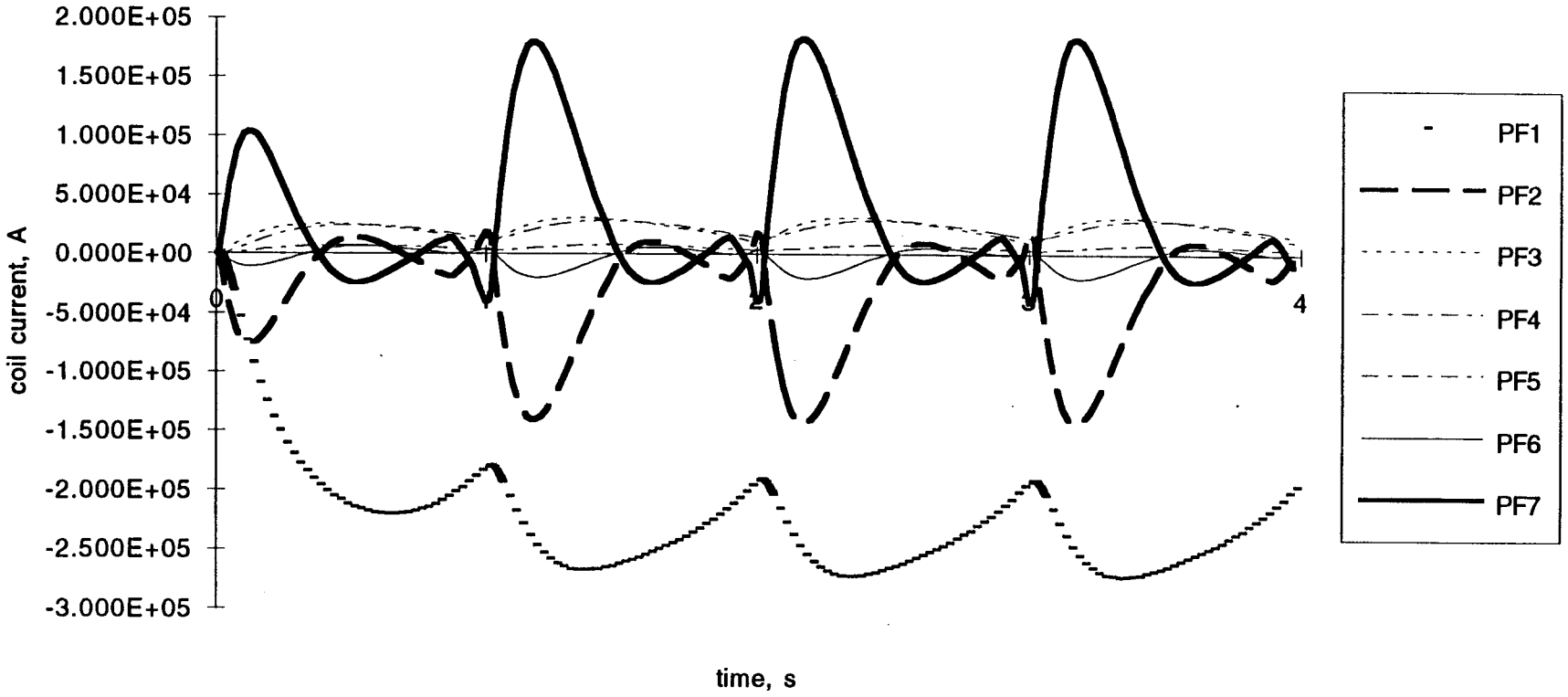

Fig. 4.1-1 ELM2 Current Simulation, Opt.#1

current versus time scenario is shown in Fig. 4.1-2. Four ELMs were modeled over a time interval of 4 seconds.

Case ELM2a :
ELM2a is defined by [10]. Coils PF2 and PF7 are active, coils PF1 and PF3-PF6 are passive and carry only the currents induced under the condition of constant flux. The current versus time scenario is shown in Fig. 4.1-3. One ELM was modeled over a time interval of 3 seconds.

Case ELM2b :
ELM2b is defined by [11]. Coils PF2 and PF7 are active, while currents in coils PF1 and PF3-PF6 are not allowed to change. The current versus time scenario is shown in Fig. 4.1-4. One ELM was modeled over a time interval of 3 seconds.

Case ELM2c :
ELM2c is defined by [12]. Coils PF2 and PF7 are active, while currents in coils PF1 and PF3-PF6 are not allowed to change. The current versus time scenario is shown in Fig. 4.1-5. Four ELMs were modeled over a time interval of 4 seconds.

In all cases the perturbation currents given were used directly without the addition of normal scenario currents.

4.2 Joule Heating of the TFCS

The Joule losses for the five cases have been calculated. The power dissipation in entire TF cold structure versus time is shown in Fig. 4.2-1 for ELM2, Fig. 4.2-2 for ELM6, Fig. 4.2-3 for ELM2a, Fig. 4.2-4 for ELM2b, and Fig. 4.2-5 for ELM2c.

The average power dissipated over the characteristic time periods are:

Case	Number of ELMs/time period	Time period (s)	Average power dissipation (W)
ELM2	3	$1 < t < 4$	1580
ELM6	3	$1 < t < 4$	4120
ELM2a	1	$0 < t < 3$	2582
ELM2b	1	$0 < t < 3$	1117
ELM2c	4	$0 < t < 4$	4144

Cases ELM2 and ELM6 show that from the point of view of minimizing the power dissipation in the TF cold structure it is preferable to use only coils PF2 and PF7 (corresponding to ELM2). In ELM6, where coils PF2-PF7 are all active, the coils close to TFCS, principally PF3-PF5, produce very high power

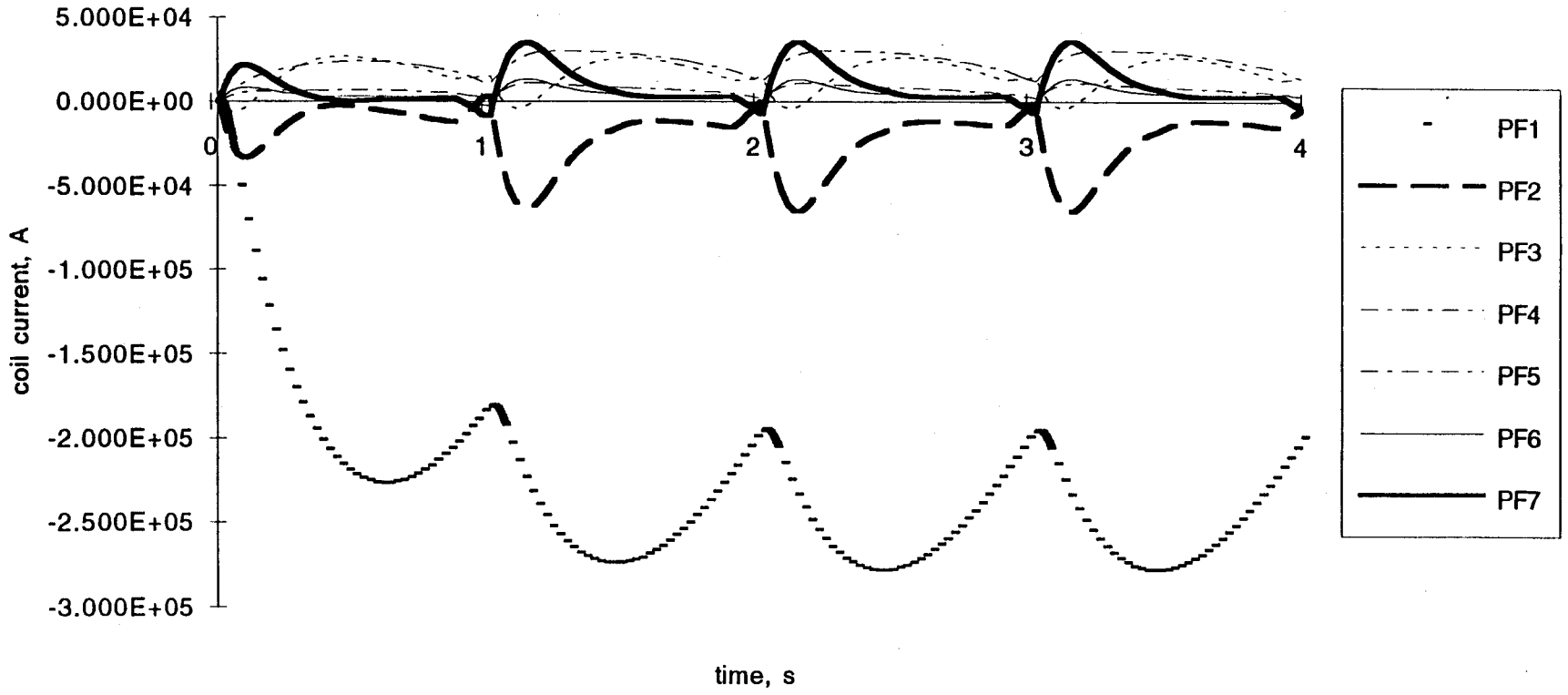

Fig. 4.1-2 ELM6 Current Simulation, Opt.#1

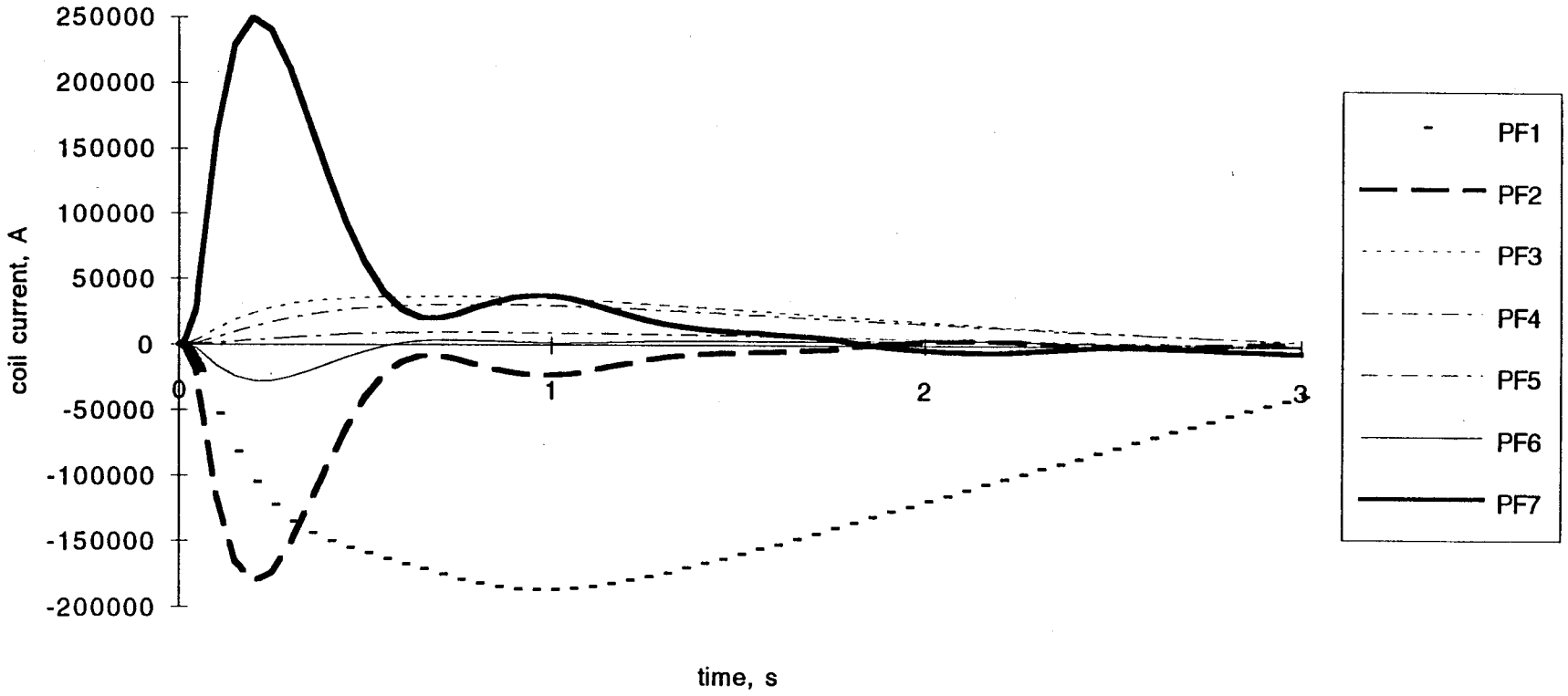

Fig. 4.1-3 ELM2a Current Simulation, Opt.#1

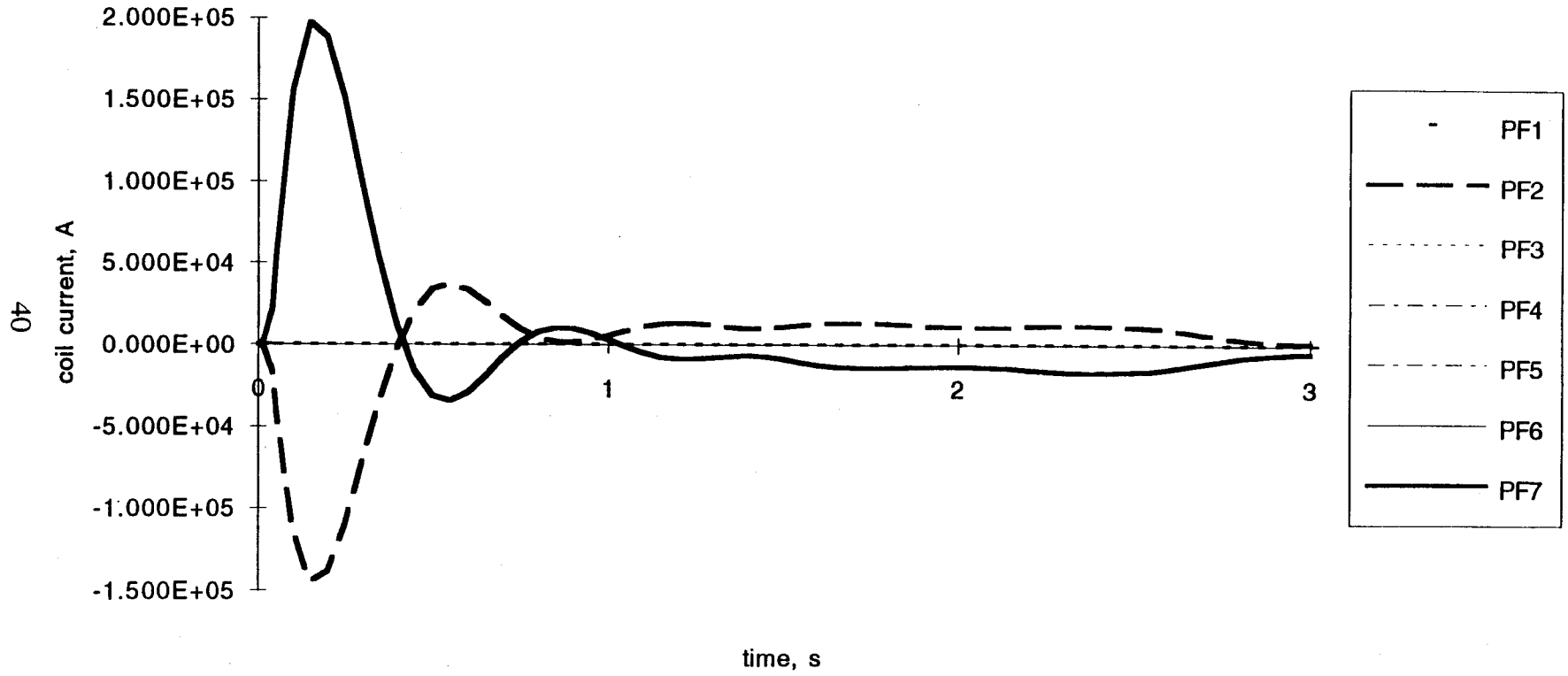

Fig. 4.1-4 ELM2b Current Simulation, Opt.#1

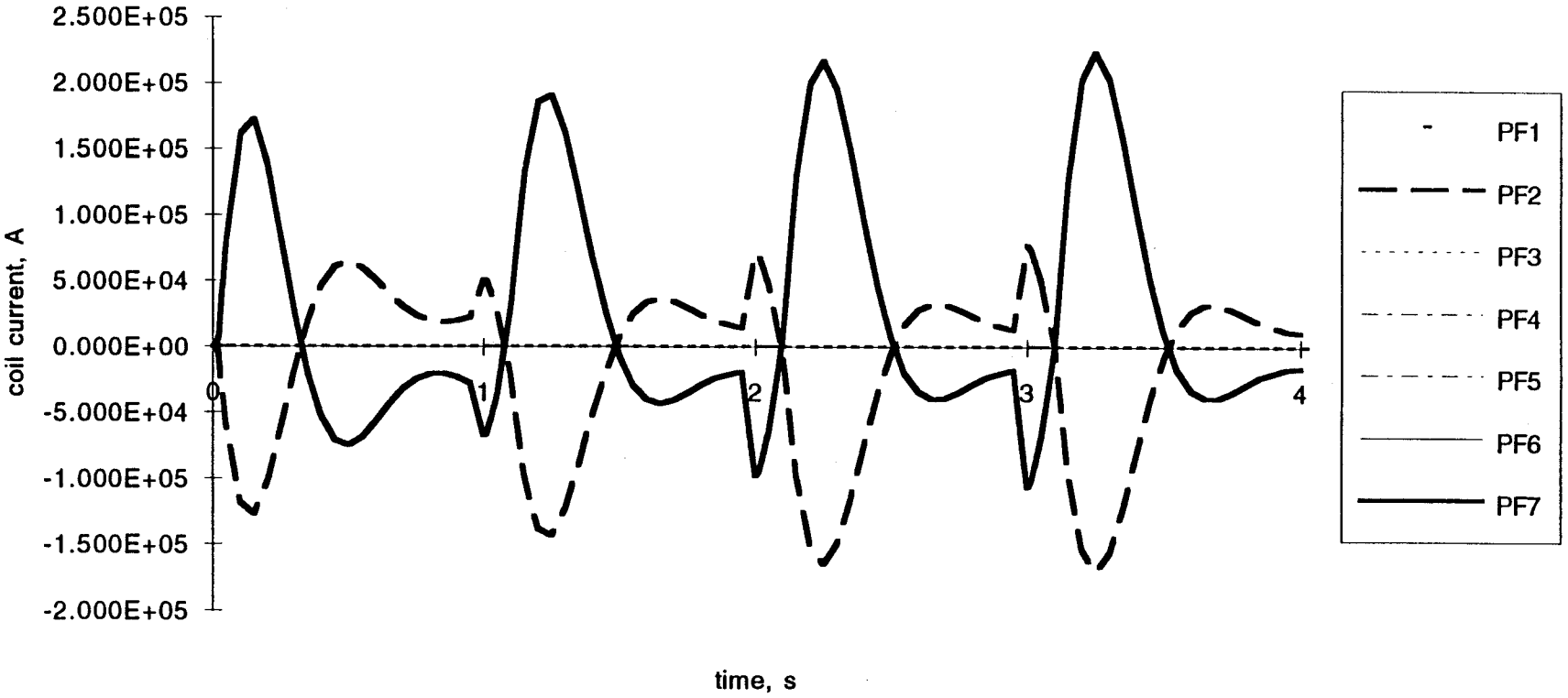

Fig. 4.1-5 ELM2c Current Simulation, Opt.#1

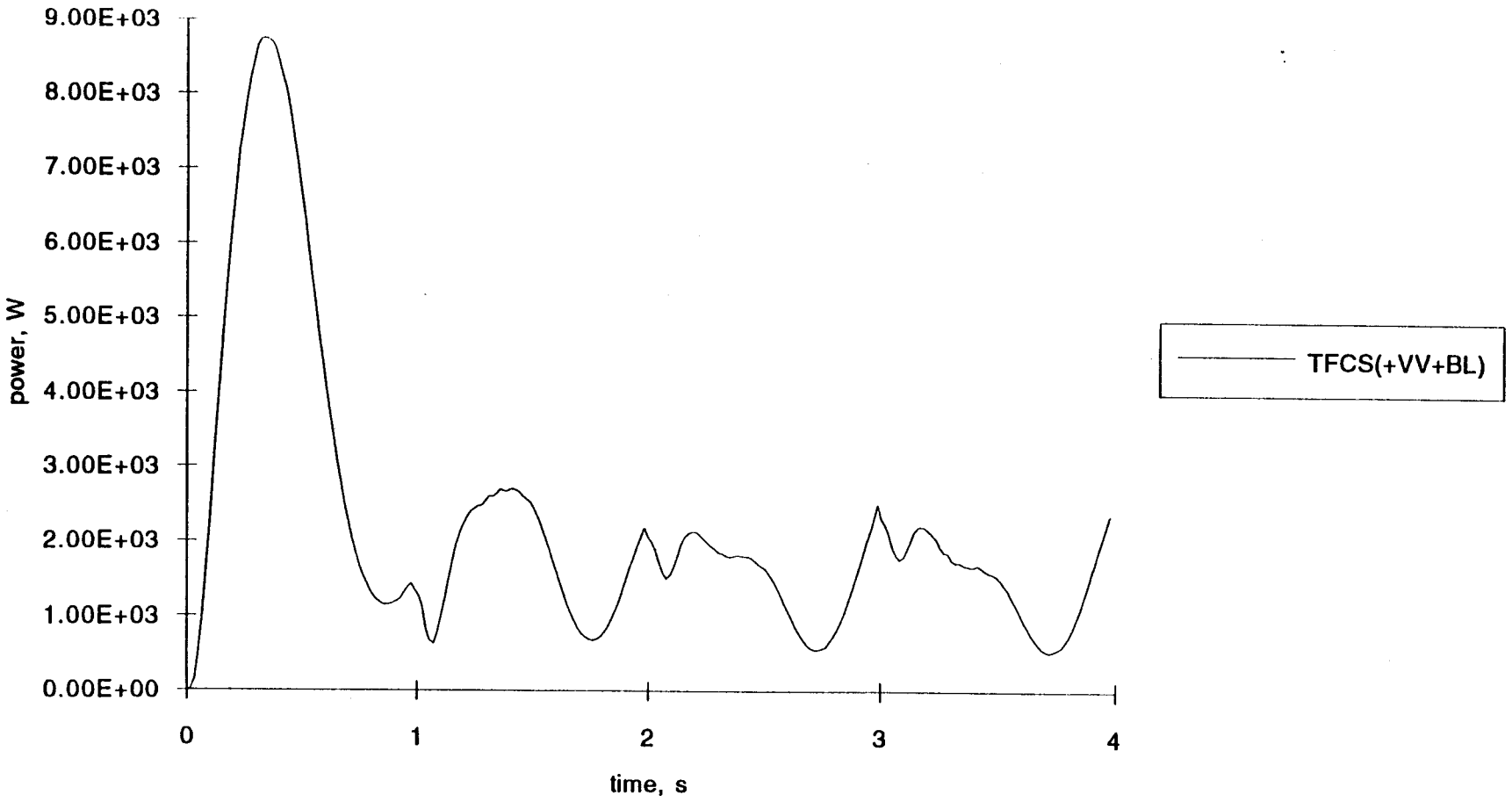

Fig. 4.2-1 Power deposition in the TFCS, Opt.#1, ELM2

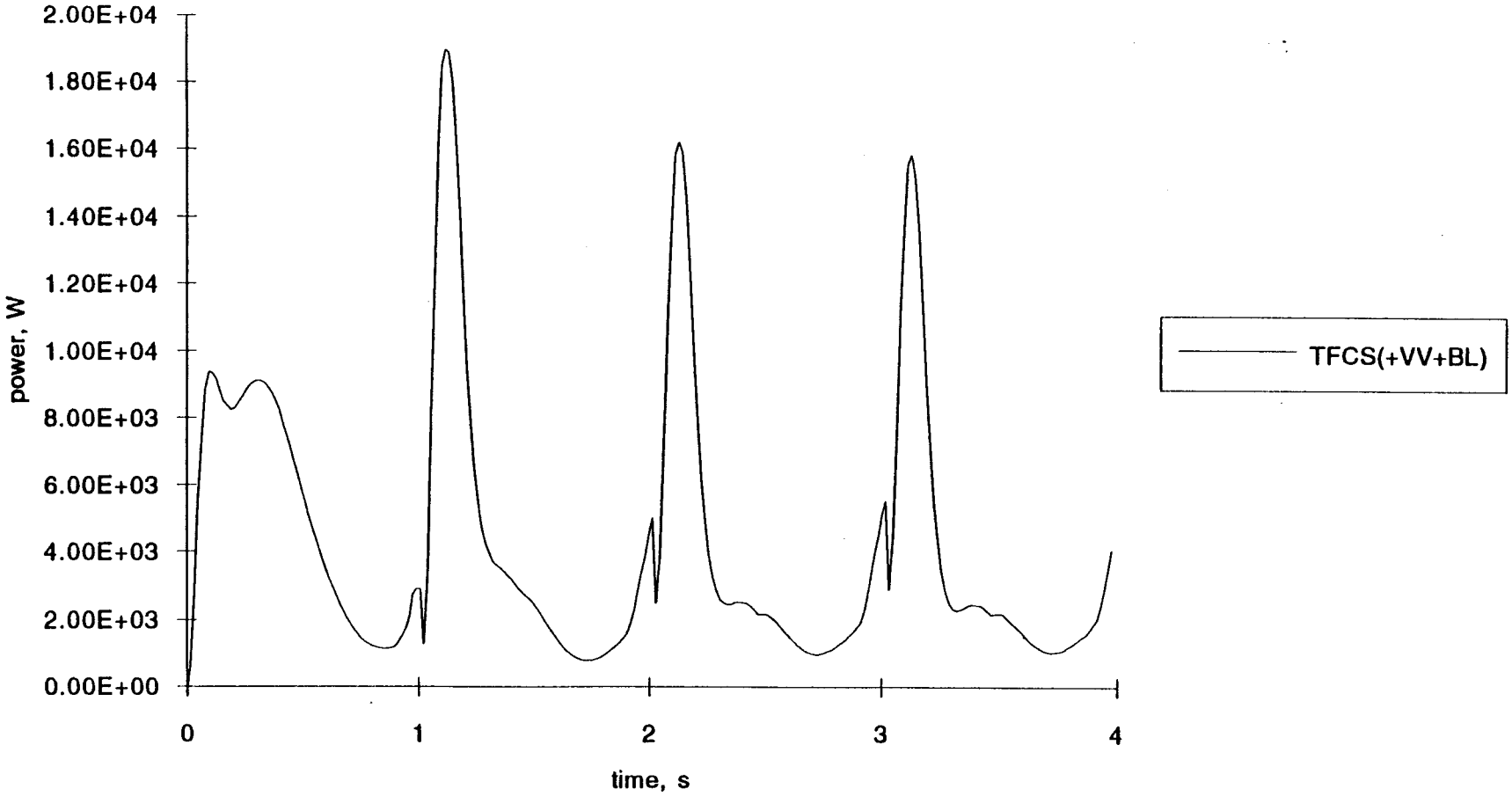

Fig. 4.2-2 Power deposition in the TFCS, Opt.#1, ELM6

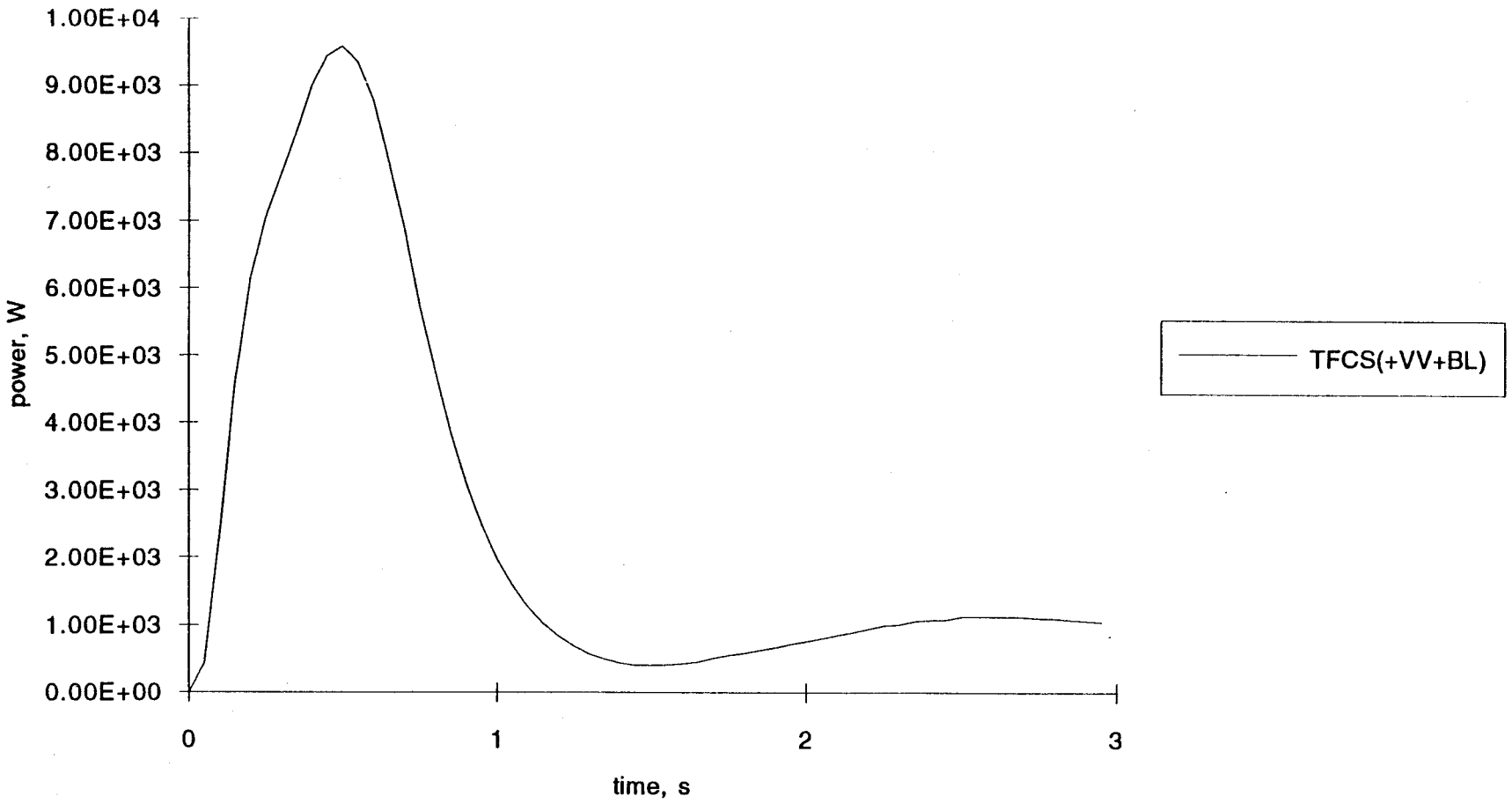

Fig. 4.2-3 Power deposition in the TFCS, Opt.#1, ELM2a

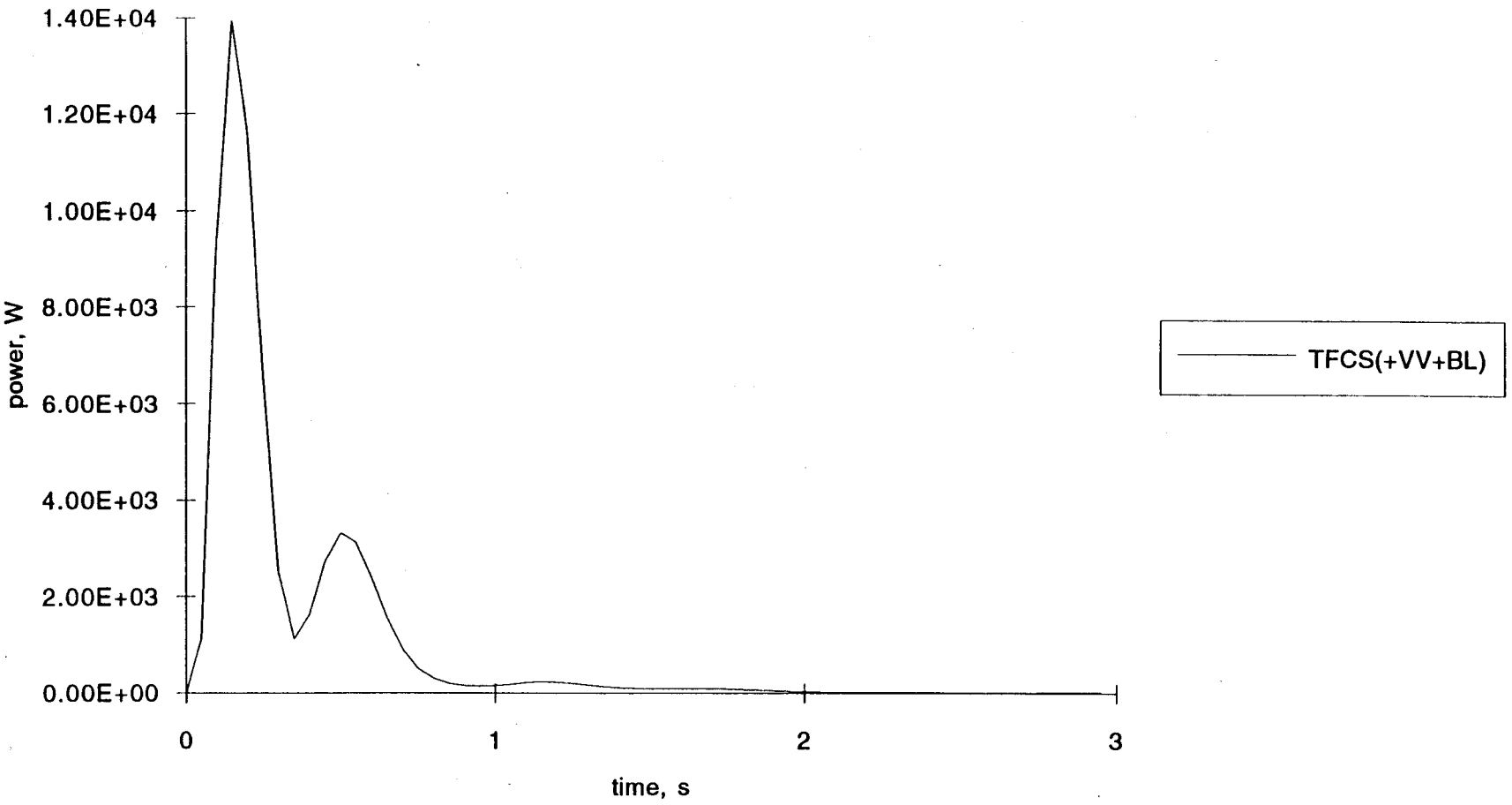

Fig. 4.2-4 Power deposition in the TFCS, Opt.#1, ELM2b

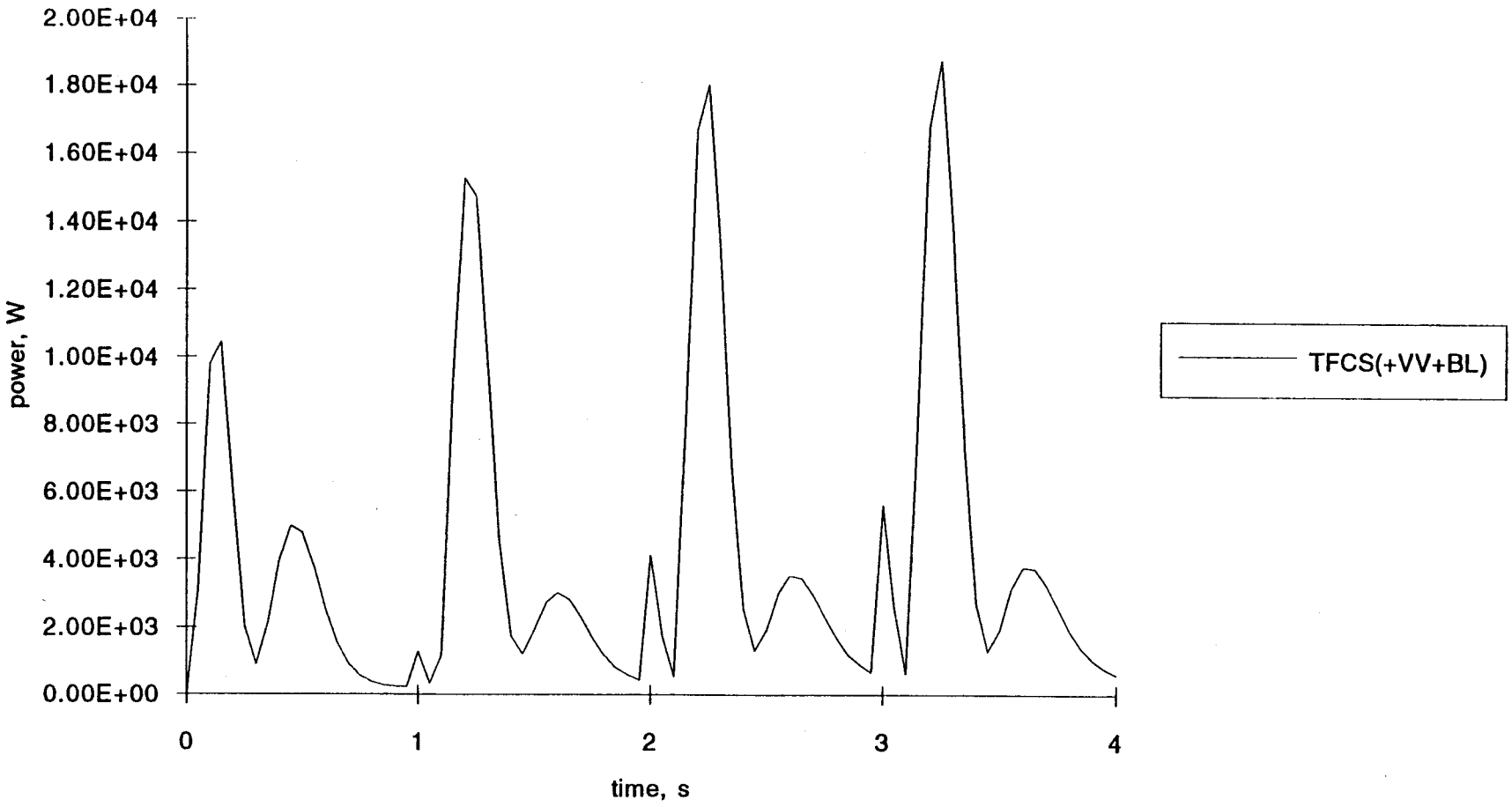

Fig. 4.2-5 Power deposition in the TFCS, Opt.#1, ELM2c

dissipation (note the high spikes in Fig. 4.2-2). In ELM2 coils PF3 and PF5 act in the opposite direction, *i.e.*, the currents induced in them cancel the flux through the TFCS due to PF2 and PF7. The eddy current patterns in the TFCS at time t=1.113 s corresponding to the spike are shown in Figs. 4.2-6 and 4.2-7 for ELM2 and ELM6, respectively. The patterns in Fig. 4.2-7 (ELM6) show a much stronger coupling between the coils and the TFCS than those in Fig. 4.2-6 (ELM2). Note the scale factor of the vectors for ELM6 is almost twice that for ELM2. Cases ELM2a-ELM2c served the purpose of confirming this suggestion.

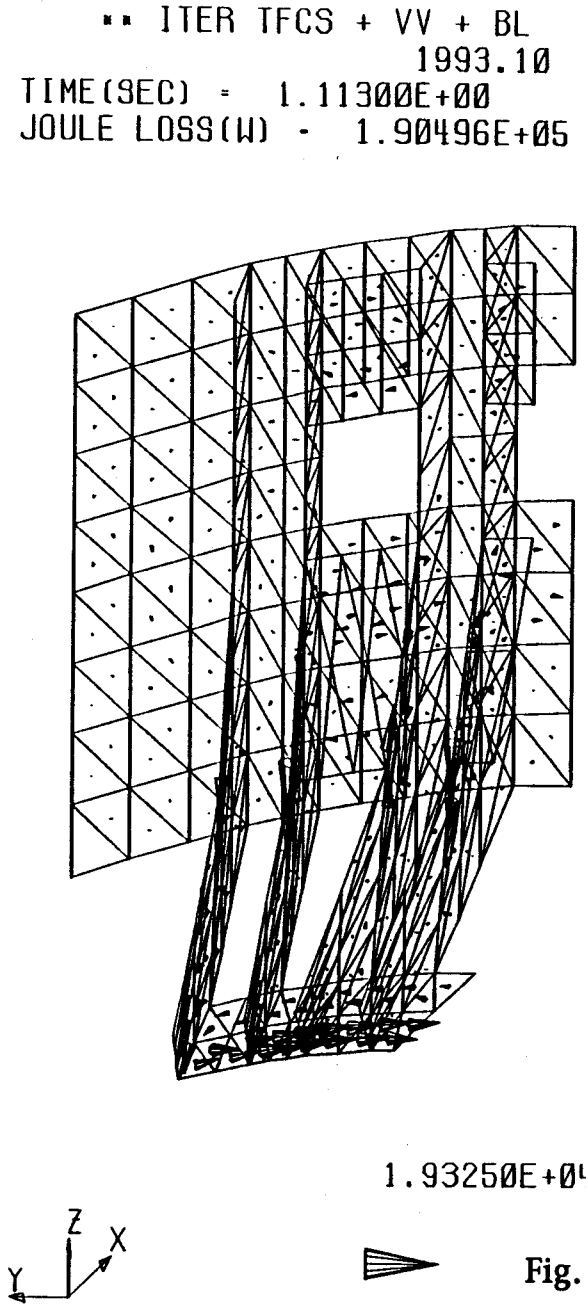

Fig. 4.2-6 Eddy currents in the TFCS, Opt.#1, ELM2

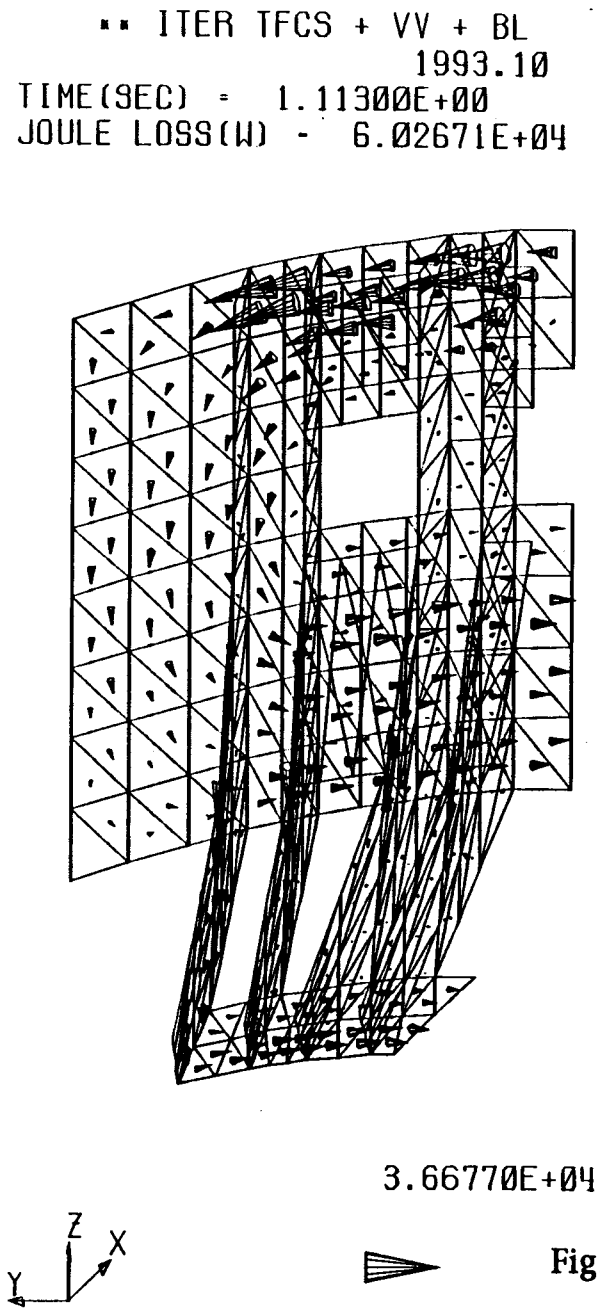

Fig. 4.2-7 Eddy currents in the TFCS, Opt.#1, ELM6

References

1. A.Kameari, "Transient Eddy Current Analysis on Thin Conductors with Arbitrary Connections and Shapes," Journal of Computational Physics, Vol. 42, No.1, July 1981, pp. 124-140.

2. NAKA CO-CENTER Fax, Ref N0.N 11 MD 01 93-07-26 F of 7-27-93.

3. Draft Design Description Document for ITER Magnet System, Ref N0.N AO RI 02 93-09-06 W.

4. R.H. Bulmer, private communication, 10-17-93.

5. R.H. Bulmer, private communication, 10-21-93.

6. R.H. Bulmer, Memorandum, "ITER Vertical Control Task, Option #2", 8-10-93.

7. R.H. Bulmer, Memorandum, "ITER Vertical Control Task, Option #3", 7-30-93.

8. L.D.Pearlstein, private communication, 10-29-93.

9. L.D.Pearlstein, private communication, 10-29-93.

10. L.D.Pearlstein, private communication, 11-1-93.

11. L.D.Pearlstein, private communication, 11-1-93.

12. L.D.Pearlstein, private communication, 11-3-93.